Dalton Transactions

Accepted Manuscript

This article can be cited before page numbers have been issued, to do this please use: M. Enel, N. Leygue, S. Balayssac, S. Laurent, C. Galaup, L. Vander Elst and C. Picard, *Dalton Trans.*, 2017, DOI: 10.1039/C7DT00291B.

This is an Accepted Manuscript, which has been through the Royal Society of Chemistry peer review process and has been accepted for publication.

Accepted Manuscripts are published online shortly after acceptance, before technical editing, formatting and proof reading. Using this free service, authors can make their results available to the community, in citable form, before we publish the edited article. We will replace this Accepted Manuscript with the edited and formatted Advance Article as soon as it is available.

You can find more information about Accepted Manuscripts in the author guidelines.

Please note that technical editing may introduce minor changes to the text and/or graphics, which may alter content. The journal's standard Terms & Conditions and the ethical guidelines, outlined in our author and reviewer resource centre, still apply. In no event shall the Royal Society of Chemistry be held responsible for any errors or omissions in this Accepted Manuscript or any consequences arising from the use of any information it contains.

ROYAL SOCIETY OF CHEMISTRY

rsc.li/dalton

View Article Online
DOI: 10.1039/C7DT00291B

New polyaminocarboxylate macrocycles containing phenolate binding units: synthesis, luminescent and relaxometric properties of their lanthanide complexes†

Morgane Enel,[a,b] Nadine Leygue,[a,b] Stéphane Balayssac,[a,b] Sophie Laurent,[c,d] Chantal Galaup,*[a,b] Luce Vander Elst*[c,d] and Claude Picard*[a,b]

[a]CNRS; Laboratoire de Synthèse et Physico-Chimie de Molécules d'Intérêt Biologique, SPCMIB, UMR-5068; 118 Route de Narbonne, F-31062 Toulouse cedex 9, France.
E-mail: picard@chimie.ups-tlse.fr (CP), galaup@chimie.ups-tlse.fr (CG)
[b]Université de Toulouse; UPS, Laboratoire de Synthèse et Physico-Chimie de Molécules d'Intérêt Biologique, SPCMIB; 118 route de Narbonne, F-31062 Toulouse cedex 9, France.
[c]NMR and Molecular Imaging Laboratory, Department of General, Organic and Biomedical Chemistry, University of Mons, 23 Place du Parc, B-7000 Mons, Belgium.
E-mail: luce.vanderelst@umons.ac.be
[d]Center for Microscopy and Molecular Imaging (CMMI), Rue Adrienne Bolland, 8, B-6041 Gosselies, Belgium

†Electronic supplementary information (ESI) available: DOSY experiments, ^{1}H NMR and MS spectra of compounds **3**, **4**, H_4L^1 and H_8L^2. HILIC-UPLC chromatograms and HMRS spectra of TbL^1, GdL^1 and Tb_2L^2 complexes. Spectroscopic characterization of Tb and Eu complexes. Influence of concentrations on the relaxation rate of GdL^1 complex.

View Article Online
DOI: 10.1039/C7DT00291B

Abstract

The synthesis of two new polyaminocarboxylate macrocycles incorporating one or two intracyclic phenol units (H_4L^1 and H_8L^2, respectively) is described. The 12-membered H_4L^1 macrocycle leads to soluble and stable mononuclear Ln^{III} complexes of $[(L^1)Ln(H_2O)_2]^-$ composition (Ln = Eu, Tb and Gd) in aqueous solutions. In Tris Buffer (pH 7.4), $[(L^1)Tb(H_2O)_2]^-$ complex displays a suitable efficiency for the sensitized emission (η_{sens} = 48%) and a high luminescence quantum yield (Φ = 22%) which is worthy of note for a bis-hydrated terbium complex. Besides, luminescence experiments show that bidentate endogenous anions (citrate, carbonate, and phosphate) do not displace the two inner-sphere water molecules of this complex. In contrast, the possible presence of LMCT states causes the europium complex to be weakly luminescent. $[(L^1)Gd(H_2O)_2]^-$ complex is characterized by a high relaxivity (r_1^{298K} = 7.2 s^{-1} mM^{-1} at 20 MHz) and a very short water residence time of the coordinated water molecules (τ_M^{298K} = 9 ns), a promising value for the conception of macromolecular systems with high relaxivities. Thus, Tb and Gd complexes of the H_4L^1 macrocycle exhibit several improvements in terms of luminescent (lower excitation energy, higher brightness) and relaxometric (shorter τ_M) properties compared to the corresponding LnPCTA complexes, where a phenol moiety substitutes pyridine ring. On the other hand, the 24-membered H_8L^2 macrocycle including two phenol units in its structure leads to dinuclear complexes of $[(L^2)Ln_2]^{2-}$ composition. Its terbium complex shows a long luminescence lifetime (2 ms) and a high quantum yield (43%) in aqueous solutions, rendering this compound a new promising candidate for time-resolved applications.

View Article Online
DOI: 10.1039/C7DT00291B

Introduction

To date various macrocyclic azaligands containing one or more phenolic groups have been designed to coordinate metal ions into their macrocyclic cavity. This is due to the higher thermodynamic and kinetic stabilities of macrocyclic chelates vs. acyclic chelates and the key role played by the phenolic moiety. This aromatic unit has several characteristics such as: (i) remarkable coordinating properties towards a large variety of ions, (ii) charge as a function of pH (0 at low pH and -1 at high pH values), (iii) interesting photoactive properties for the access of optical sensors, (iv) capability for binding two metal centres in a bridge position, allowing stabilization of dinuclear species, (v) a benzene ring allowing a great synthetic flexibility. Macrocyclic ligands containing phenolic unit(s) have been largely used in transition-metal complexes[1] but have received less attention as lanthanide chelators. Moreover, the physicochemical properties of Ln^{III} complexes formed by this type of ligands are essentially reported in the solid state or in organic solutions.[2] For example, Nakai et al. demonstrated recently that terbium^{III} complexes derived from tacn (1,4,7-triazacyclononane) and cyclen (1,4,7,10-tetraazacyclododecane) platforms bearing three and four phenol pendant arms, respectively, are highly oxygen sensitive luminescent probes, but operating only in THF solutions.[2a,b] The literature regarding the incorporation of phenolic function into macrocyclic ligands able to complex Ln^{III} ions in aqueous solutions is very limited. Sherry used a gadolinium complex based on a DO3A core (DO3A = 1,4,7,10-tetraazacyclododecane-1,4,7-triacetic acid) with a p-nitrophenolic pendant arm as a pH-responsive MRI contrast agent.[3] The luminescence properties of a dinuclear europium complex derived from two DO3A units separated by a p-nitrophenolic group were highlighted very recently by Faulkner.[4] We can also note that Bünzli and co-workers briefly reported the photophysical and relaxometric properties of mono-aqua lanthanide iminophenolate cryptates.[5]

In the course of our research on the design of Ln^{III} complexes acting as luminophores and paramagnetic contrastophores by simple permutation of the lanthanide ion,[6] we were interested in the development of a new macrocyclic chelator derived from the DOTA backbone (DOTA = 1,4,7,10-tetraazacyclododecane-1,4,7,10-tetraacetic acid) where a phenolic unit is substituted for a dimethylene aminoacetate moiety (ligand H_4L^1, Fig. 1). In this structure, the diethylenetriaminetriacetic acid core is an efficient chelating system for Ln^{III} ions in aqueous solutions. Since Ln^{III} ions exist as a hydrated aqua ion with ~8-9 inner-sphere water molecules below pH ~ 6 in aqueous solutions, the heptadenticity of this ligand

View Article Online
DOI: 10.1039/C7DT00291B

allows the coordination of one or two water molecules in the inner-sphere of Ln^{III} complexes. On the one hand, this structural parameter fulfils the requirement of Gd-based relaxation agents, where the metal centre catalytically shortens the longitudinal (T_1) relaxation times of nearby water protons. In these systems, it is well known that di-aqua Gd^{III} complexes possess an intrinsically higher relaxivity than those complexes of similar size with a hydration state of 1.[7] On the other hand, the presence of a metal hydration state in luminescent lanthanide complexes implies non radiative deactivation pathways associated with energy transfer between Ln^{III} excited states and OH oscillators.[8] Nevertheless, in some cases di- or tri-aqua terbium complexes can display interesting photophysical properties.[9] Moreover, the phenolic unit is able to promote the so-called "antenna effect" where light absorbed by the organic ligand is transferred *via* singlet and triplet states to the excited resonant levels of the lanthanide ions.[10] Prior to this work, Natrajan et al. reported the structure and spectroscopy behaviour of Tb^{III} complex with a closely related acyclic ligand, H_5(5-Me-HXTA) (Fig. 1).[11] In aqueous solutions, this complex exists as unusual discrete dimeric pairs (M_2L_2 species; M = Tb, L = 5-Me-HXTA) and no water molecule are coordinated to the two metal ions. It displays a luminescence quantum yield of around 50% which is among the highest reported in aqueous solutions for Tb^{III} complexes.

In this contribution, we report the synthesis of the 12-membered macrocycle H_4L^1 and its corresponding dimeric 24-membered macrocycle H_8L^2. A detailed photophysical study in aqueous solutions of the mononuclear LnL^1 and dinuclear Ln_2L^2 complexes (Ln = Eu^{III}, Tb^{III}) was undertaken to help us better understand the role played by the various factors that determine their luminescence properties. Since we showed that the LnL^1 complexes are able to coordinate two water molecules, we have also investigated the relaxation properties of the GdL^1 complex in aqueous solution by ^1H relaxometry and ^{17}O NMR. Attention was also paid to the kinetic stability of bis-hydrated LnL^1 complexes towards bidentate anions interactions and transmetallation process with Zn^{2+} ions. Finally, comparison to the parent Ln^{III} PCTA complexes containing a pyridinic intracyclic unit[12] and Gd^{III} DOTA allowed us to evaluate the influence of a phenol moiety on the luminescent and relaxometric properties of 12-membered macrocyclic Ln^{III} complexes.

Results and discussion

Synthesis

View Article Online
DOI: 10.1039/C7DT00291B

Our synthetic strategy for the preparation of H_4L^1 was based on the use of unprotected phenol derivative and a linear triamine bearing *tert*-butyl acetate pendant groups (Scheme 1). This triamine **1** may be prepared in three steps from commercially available diethylenetriamine following our previously reported procedure (overall yield: 74%).[13] Using these synthons avoids harsh conditions generally required for deprotection of phenolic ethers and the need of a N-carboxyalkylation step on polyamine macrocycles.[14] As reported in the literature, the use of a 2-fold aminomethylation reaction implying iminodiacetate derivatives/paraformaldehyde with substituted phenols is the route of choice to have access to corresponding acyclic ligands.[11,15] In this context, we initially attempted the synthesis of macrocycle **3** via mannich reaction between *p*-cresol and triamine **1**. However this synthetic route proved unsuccessful and only the formation of acyclic intermediate products was observed from numerous attempts. Our efforts were then turned towards a classical direct alkylation of bis(halomethyl) phenol on triamine **1**. Condensation of 2,6-bis(bromomethyl)-4-methyl-phenol with triamine **1** was carried out in acetonitrile at reflux and in the presence of sodium carbonate as a base and without using high-dilution technique (reactants concentration 2×10^{-3} M). ^{1}H NMR DOSY analysis of the crude mixture showed the presence of only two species which display translational diffusion coefficients (D) relative to $CDCl_3$ of 710 and 560 $\mu m^2 s^{-1}$ (Fig. 2). The positive electrospray mass spectrum established the formation of both the 12-membered monomer structure **3** ($[H_4L^1+H]^+$ at m/z = 578.4, 100%) and the corresponding 24-membered dimer structure **4** ($[H_8L^2+H]^+$ at m/z = 1155.7, 100%). After purification by column chromatography on alumina, macrocycles **3** and **4** were isolated in 31 and 55% yields, respectively. Although no polymeric species was detected in this macrocyclization process, the 1:1 cyclization reaction is not promoted with respect to the 2:2 process by a sodium "template″ effect. Besides, changing the nature of the alkaline carbonate has noticeable effects on the monomer-dimer distribution in this macrocyclization reaction. Under similar reaction conditions, the ratio of monomer/dimer selectivity (R) is increased by a factor of 4.8 by replacing sodium carbonate (R = 0.56) by lithium carbonate (R = 2.7). Other alkaline carbonate (K_2CO_3 and Cs_2CO_3) favour the production of the dimeric species but is accompanied by a higher formation of by-products. The more favourable formation of the monomer [1 + 1] macrocycle in the presence of the lithium cation may be attributed to a better fit of this ion with the macrocyclic cavity. It is worth noting that these 12-membered and 24-membered macrocycles **3** and **4** can be readily distinguished by ^{1}H NMR spectroscopy (Fig. 2 and ESI Fig S1 and S2[†]). Their ^{1}H NMR spectra display significant difference,

View Article Online
DOI: 10.1039/C7DT00291B

reflecting some rigidity of the monomeric species and a more fluxional system for dimeric species. Compound **3** displays AX and AB spin patterns for pseudo benzylic protons (J =12.9 Hz) and methylenic protons of the two lateral ester arms (J =16.8 Hz), respectively, a singlet for the central arm and three signals for the remaining macrocyclic protons in the 2.03 – 2.92 ppm range. The ^{1}H NMR spectrum of **4** shows only four sets of signals for the methylenic protons. Subsequent acid hydrolysis (HCl, rt) of the *tert*-butyl ester functionalities afforded the ligands H_4L^1 and H_8L^2 as hydrochloride salts in good yields (See ESI, Fig. S3 and S4[†]).

The stoichiometry of the Tb^{III} complexes formed with H_4L^1 and H_8L^2 were determined by a mol ratio method. By monitoring the Tb^{III} luminescence as the function of Tb^{III} added to an aqueous solution of ligands (Tris buffer, pH 7.4), binding curves were obtained (Fig. 3). The total integrated intensity of the emission increased upon Tb addition up to one equivalent (H_4L^1) and two equivalents (H_8L^2), after which a plateau in the emission intensity was reached. These data are consistent with the formation of a single complex species with a 1:1 ligand-to-lanthanide stoichiometry for ligand H_4L^1 and a 1:2 stoichiometry for H_8L^2. The ESI$^-$-MS spectra obtained with aqueous solutions containing H_4L^1 or H_8L^2 and Tb^{3+} in a ratio 1:1 or 1:2, respectively, are in agreement with the results of luminescence titrations. These spectra are characterized by the presence of base peaks corresponding to one or two negatively charged species ($[TbL^1]^-$ or $[Tb_2L^2]^{2-}$, supporting the formation of mono- or di-nuclear complexes. Consequently, the Ln^{III} (Ln = Eu, Tb, Gd) chelates derived from these ligands were prepared at room temperature in aqueous solutions with an appropriate slight molar excess (ca. 10%) of the lanthanide salts ($LnCl_3.6H_2O$) to avoid the presence of free ligands. After purification (Waters sep-pack® cartridge C18), no peaks ascribable to the free ligand were found in the ESI mass spectra and HILIC-UPLC analyses of the complexes (See ESI, Fig. S5-S7[†]). Yields were quantitative. Interestingly, the Eu^{III}, Gd^{III} and Tb^{III} complexes showed identical UPLC retention times within their respective series (L^1 and L^2), suggesting that Ln^{III} ions share the same coordination sphere for each complexes series.

Photophysical properties of TbL^1 and Tb_2L^2 complexes

The main electronic and photophysical properties of the two Tb^{III} complexes are given in Table 1, together with analogous data of other relevant Tb^{III} complexes for comparison. Their UV-Vis spectra are similar, displaying two absorption bands at 242 and 296 nm in air equilibrated Tris buffer (50 mM, pH 7.4). When compared to TbPCTA, the sensitizer

View Article Online
DOI: 10.1039/C7DT00291B

phenolate induces a shift of the lowest-energy absorption band towards lower energy (red shift of 27 nm).

At room temperature, the emission spectra of TbL^1 and Tb_2L^2 show typical narrow-band lanthanide luminescence in the visible region after excitation into the lowest-energy absorption band of the two ligands (λ_{exc} = 296 nm) (Fig. 3). These emission bands at 490, 545, 586 and 622 nm, with weaker signals in the 640-700 nm were assigned to the $^5D_4 \rightarrow {}^7F_J$ (J = 0-6) transitions of Tb^{III} ion.[16] In both cases, the sensitive $^5D_4 \rightarrow {}^7F_5$ transition at 545 nm is the most prominent and accounts for ~ 55% of the total integrated emission intensity. As expected, the absorption and excitation spectra overlap well, which confirms the sensitized character of the observed emissions (See ESI, Fig. S8†).

More insight in the nature of the coordination sphere of the Tb^{3+} centre may be obtained from the emission lifetimes. For the two complexes, luminescence decays are monoexponential functions, suggesting the presence of a single emissive solution species in each complex and the presence of two metal sites with very similar environment in Tb_2L^2. At room temperature, the emission lifetime of the $^5D_4$ level are 1.16 and 2.02 ms with TbL^1 having the shortest value. From the lifetime data in the deuterated and non-deuterated water, calculation of the number of metal-bound water molecules (q) was possible, owing to the well-established isotope effect[17] and by using the empirical relationship developed by Beeby et al.[18] This analysis indicated that two water molecules are present in the first coordination sphere of the metal in TbL^1, whereas no water molecules are present in the case of Tb_2L^2 (Table 1). If the determination of the hydration sphere of the metal assesses the extent of the radiationless deactivation of Tb(III) excited states by OH oscillators, this value is also suggestive of the number of remaining atoms in the first coordination sphere as Tb^{3+} prefers a coordination number of 8-9 in aqueous solutions.[19] Assuming that the ligand H_4L^1 is heptadentate, these results are fitting in well with a nine-coordinated TbL^1 complex. The absence of coordinated water molecules in Tb_2L^2 leads us to suppose that the two metal ions are bridged by each μ^2-PhO phenolate moiety, leading to an overall coordination number of 8 for each terbium ion (Fig. 4). Such behaviour has been observed in the solid state and in solution for the 2:2 dimeric complex $[Tb(5\text{-Me-HXTA})]_2$.[11] On the other hand, no concentration effects were observed for TbL^1. The measurement of the luminescence lifetime over a concentration of 10^{-6} to 10^{-3} M led to monoexponential fitting of the decay curves and to τ values constant within error (1.16 ms), in agreement with the presence of a single emissive species with two inner-sphere water molecules and the preservation of a mono-nuclear structure. From the data

View Article Online
DOI: 10.1039/C7DT00291B

reported in Table 1, we can notice that lifetimes in D_2O solutions at 298 and 77 K are similar for both complexes. This result shows that temperature-dependant non-radiative decay processes, such as a back-energy transfer from the metal-centred level to the ligand-centred triplet level which is observed particularly for Tb complexes, do not occur.

As well established, the energy levels of the ligand excited states play a leading role in the intramolecular energy transfer process (L* $\rightarrow$ Ln*).[20] Hence, we investigated as usual the behaviour of these ligand-centred (LC) levels in the corresponding Gd^{III} complexes (Fig. 5). In Tris buffer and at room temperature, the emission spectrum of GdL^1 is dominated by a broad emission band with a peak maximum at 338 nm after excitation at 296 nm. The relatively small Stokes shift (ca. 4200 cm^{-1}) and the fact that the intensity of the observed emission band vanishes when a short delay (10 μs) is enforced led us to assign this band to $^1\pi\pi^*$transitions. A similar fluorescence emission band (λ_{em} = 345 nm, λ_{exc} = 290 nm) was reported for the anionic phenol in aqueous solution.[21] At low temperature (77 K) in a 4:1 Tris buffer-glycerol glass, a second emission band is observed with a maximum around 405 nm and a single-exponential time decay with a lifetime of 1.48 ms. On the bases of its energy level and long-living excited states, this emission is attributed to $^3\pi\pi^*$transitions. From these experiments, the energy of the 0-0 transition of the first excited singlet state of GdL^1 was estimated to be 32500 cm^{-1} (intercept of the absorption and fluorescence spectra) and the value of the 0-0 energy for the ligand triplet state was estimated to be 26000 cm^{-1} (shoulder at 385 nm in the phosphorescence spectrum). The calculated energy for T_1 in GdL^1 is consistent with previous reports of the phenol T_1 energy level by Latva et *al.* (26600 cm^{-1}) in 5-Me-HXTA and Nakai et al. (26460 cm^{-1}) in $[Gd(^{MeMe}ArO)_3tacn]$.[2a,22] Similar energies for S_1 and T_1 excited states (32700 and 26500 cm^{-1}, respectively) were observed for Gd_2L^2. For the two investigated complexes, the energy gaps ΔE ($^1\pi\pi^* - {}^3\pi\pi^*$) and ΔE ($^3\pi\pi^* - {}^5D_4$) amount to 6200/6500 and 5500/6000 cm^{-1}, respectively. These data are in accordance with the empirical rules for effective intersystem crossing, ISC, (ΔE ($^1\pi\pi^* - {}^3\pi\pi^*$) < 7000 cm^{-1}) and irreversible energy transfer between the antenna triplet state and the Tb^{III} $^5D_4$ state (ΔE ($^3\pi\pi^* - {}^5D_4$) > 2000 cm^{-1}).[23,24]

Overall quantum yields (Φ_{ov}) of TbL^1 and Tb_2L^2, defined as the ratio between the number of photons emitted by the Ln^{III} ion and the number of photons absorbed by the ligand, were determined experimentally by excitation of the ligand (λ_{exc} = 296 nm) in aerated Tris buffer (pH 7.4) and at room temperature. Despite the presence of two coordinated water molecules the luminescence quantum yield of TbL^1 remains very interesting in H_2O solution with a 22%

View Article Online
DOI: 10.1039/C7DT00291B

value and is significantly larger than that of bis-hydrated complex TbPCTA (8.3%). Besides, Tb_2L^2 displays a quantum yield (43%) higher or close to the ones reported for terbium-based commercial luminescent probes (32% for Tb(DTPA-Cs124) and 50% for Tb(Lumi4^{TM})).[25] It is also interesting to note that this quantum yield is close to that reported for the corresponding dinuclear complex $[Tb(5\text{-Me-HXTA})]_2$. In D_2O solution the quantum yields of TbL^1 and Tb_2L^2 are similar and consistent with the dependence of the luminescence quantum yields of Tb^{III} complexes as a function of the lowest triplet state energy of the ligand, proposed by Latva et al.[24] To our knowledge, this is only the second report of luminescence properties in aqueous solutions of a dinuclear Tb^{III} complex derived from a macrocyclic ligand.[26] In a second step, the Φ_{ov} values for TbL^1 and Tb_2L^2 complexes have been analyzed in terms of eqn (1) which takes into account the multistep pathway of an antenna effect.[8]

$$\Phi_{ov} = \eta_{sens} \times \Phi_{Tb} \qquad \text{eqn (1)}$$

In this equation, η_{sens} corresponds to the sensitization efficiency which is mainly reflecting ISC and energy transfer from the ligand-centred triplet state to the lanthanide ($\eta_{sens} = \Phi_{ISC} \times \eta_{ET}$) and Φ_{Tb} the intrinsic quantum yield, i.e. the quantum yield by direct excitation of the lanthanide ion. Assuming that the decay process at 77 K in a deuterated solvent is purely radiative, Φ_{Tb} can be estimated through eqn (2).[10, 27]

$$\Phi_{Tb} = \tau_{obs}^{298K}(H_2O) / \tau_{obs}^{77K}(D_2O) \qquad \text{eqn (2)}$$

As can be seen in table 1, the sensitization efficiency, that is independent of the presence of inner-sphere water molecule, is comparable for the two complexes (~ 50%), indicating a rather efficient sensitization process. TbL^1 and Tb_2L^2 have close-lying energies of both the ligand singlet and triplet states, this suggests equivalent Φ_{ISC} and that the energy transfer efficiency η_{ET} does not depend on the $^3\pi\pi^* \rightarrow Ln^*$ energy gap. As the efficiency of Förster energy transfer from the antenna to the lanthanide follows an r^6 dependence, it is likely that similar chromophore – metal distance occurs in these two different structures. On the other hand, the ligand-to-metal energy transfer process is sensitive to the replacement of a pyridine moiety with phenol moiety, increasing η_{sens} by a factor of 2.4 from TbPCTA to TbL^1. Since Φ_{Tb} is similar for these two complexes, the difference in their Φ_{ov} values is due to the difference in sensitization efficiency.

The emission properties of these Tb^{III} complexes in aerated solutions at room temperature remained unchanged for several days in Tris buffer (pH 7.4), which highlights their stabilities in aqueous media. On the other hand, Tb_2L^2 is more resistant than TbL^1 to transchelation in the presence of DTPA, a competing ligand which binds strongly to Tb^{III} (K(TbDTPA) = 5.1

View Article Online
DOI: 10.1039/C7DT00291B

10^{22}).[28] In the presence of one equivalent of DTPA and based on luminescence experiments, 8.5% of Tb_2L^2 and 77% of TbL^1 were dissociated after 24h in Tris buffer (pH 7.4). The weaker kinetic inertness of TbL^1 could be related to the presence of two water molecules in its first coordination sphere. Nevertheless, in the same experimental conditions, the bis-hydrated TbPCTA complex was only 6% dissociated. Further potentiometric studies would have to be performed in order to gain a quantitative understanding of the stability of these complexes.

The partial or complete displacement of the inner-sphere water molecules by bidentate endogenous anions (phosphate, carbonate, *L*-lactate) has often been observed for bis-hydrated lanthanide complexes.[29] In this direction, we investigated this behaviour for the TbL^1 complex by luminescence spectroscopy. If one or both water molecules are indeed replaced by these oxoanions, the luminescence intensity and lifetime will increase. TbL^1 complex (50 μM) was challenged in Tris buffer by a great excess of these anions in relation to their physiological concentrations in human plasma (phosphate, 1.1 mM; carbonate, 26 mM and L-lactate, 2.3 mM).[30] Addition of phosphate caused no changes in the observed emission intensity, while addition of citrate or carbonate caused a small variation (~ 10%) in intensity. In all three cases, the slight increase of emission lifetimes ($1.17 < \tau < 1.25$ ms) is consistent with the retention of the two coordinated water molecules and therefore the absence of interaction between TbL^1 and these dianions, in a mono- or bidentate manner. In the same experimental conditions, a similar behaviour was observed with TbPCTA (See ESI, Fig. S9†). In these two complexes, the relative position of the two first-shell water molecules is certainly not adapted for bidentate interactions. In DO3A-type complexes, the water molecules are adjacent in the coordination polyhedron allowing a bidentate binding of these anions. We have also studied the displacement of inner-sphere water molecules by small-hard charged F^- anions in TbL^1 and TbPCTA complexes. This effect has been successfully exploited in sensitized luminescent Ln^{III} systems, reducing the H_2O quenching.[31] In the presence of a saturating anion concentration (0.1 M, F^-), the luminescence lifetime is increased by a factor of 1.08 (TbL^1) and 1.57 (TbPCTA). The displacement of water from the coordination sphere of the metal is thus more marked for TbPCTA. The presence of an overall negative charge of TbL^1, limiting electrostatic interactions between Tb^{III} and F^- ions, could explain this result.

Photophysical properties of EuL^1 and Eu_2L^2 complexes

At room temperature, excitation into the ligand levels of EuL^1 and Eu_2L^2 complexes results in characteristic emission of Eu^{III} ion in the visible region (500 – 800 nm) with the strongest

View Article Online
DOI: 10.1039/C7DT00291B

emission based on the $^5D_0 \rightarrow {}^7F_2$ transition occurring at 616 nm (See ESI, Fig. S10†). The triplet energies of the two investigated ligands (26000/26500 cm^{-1}) are suitable to give rise to energy transfer to the accepting levels of the Eu^{III} ions (17500 $cm^{-1} \leq E\ ^5D_J$ (J = 0-3) $\leq$ 24500 cm^{-1}), but only weak lanthanide-based luminescence was observed from these Eu^{III} complexes in contrast to the results for TbL^1 and Tb_2L^2. EuL^1 and Eu_2L^2 complexes are characterized by very low quantum yields, 0.03% and 0.55% respectively, in comparison with that of EuPCTA (4.3%). These very weak metal-based emissions may be rationalized by the presence of nonradiative LMCT (ligand-to-metal charge-transfer) states, as might be expected with the low reduction potential of the Eu^{III} ion and an electron donating phenolate antenna group.[11,32,33] These LMCT transitions are tentatively assigned in the UV-vis absorption spectra as a tail of the lowest-energy absorption band (at 360 nm, ε = 80 and 260 $dm^3\ mol^{-1}\ cm^{-1}$ for EuL^1 and Eu_2L^2, respectively (See ESI, Fig. S11†)).[11] At room temperature, the luminescence lifetime of EuL^1 is 0.31 ms, similar to EuPCTA (τ = 0.37 ms) and typical of bishydrated Eu^{III} complexes. Besides, the τ value of Eu_2L^2 is 0.55 ms and lies in the lower range of those usually observed for Eu^{III} complexes with no inner-sphere water molecules. A similar lifetime value was reported recently for an europium complex derived from a nonadentate picolinate ligand.[34] Finally, luminescence lifetimes of EuL^1 and Eu_2L^2 measured in deuterated aqueous solutions (τ_D = 0.87 and 0.70 ms, respectively) confirm the hydration number observed for the corresponding Tb^{III} complexes.

Relaxometric studies of GdL^1 complex.

The relaxometric properties of GdL^1 were first assessed by measuring its overall relaxivity r_1 which represents the increase in the longitudinal nuclear magnetic relaxation rate of water protons promoted by the paramagnetic complex. For comparison purpose, this parameter is commonly measured for a millimolar solution of the Gd^{III} complex in water at pH 7, at 20 MHz and 298 or 310 K. In these conditions, the relaxivity of GdL^1 is 7.2 and 5.7 $s^{-1}\ mM^{-1}$ at 298 and 310 K, respectively. These values are clearly higher than those of mono-aqua Gd^{III} complexes, currently clinically used MRI CAs (r_1^{310} = 3.5 - 3.8 $s^{-1}\ mM^{-1}$ at 20 MHz).[35] On the other hand, they are in the range of those reported for other di-aqua Gd^{III} complexes of small size with relaxivities ranging from 5.7 to 10.2 $s^{-1}\ mM^{-1}$ at 20 MHz and 298 K.[36] Besides, we can note that the value of 5.7 $s^{-1}\ mM^{-1}$ is slightly higher than that of the parent GdPCTA complex where a pyridine ring is substituted for a phenol moiety (r_1^{310} = 5.4 $s^{-1}\ mM^{-1}$).[37] The

View Article Online
DOI: 10.1039/C7DT00291B

presence of two water molecules in the first coordination sphere of the GdL^1 complex was confirmed by the measurement of the O-17 chemical shift of GdL^1 as compared to that of Gd-DOTA for which q=1. A value of 1.75 was obtained in good agreement with the value obtained by photophysical measurements of the corresponding Tb and Eu complexes.

In addition to the hydration state, the residence time (τ_M) or the corresponding exchange rate ($k_{ex} = 1/\tau_M$) of water molecules in the inner-coordination sphere of a gadolinium ion and the tumbling motion of the complex (τ_R) contribute to the overall relaxivity of a Gd^{III} chelate.[38] There are several well established physico-chemical methods to determine these two parameters.[39] The quantitative evaluation of τ_M can be carried out through the analysis of the temperature dependence of the reduced transverse ^{17}O relaxation rate of water ($^{17}O–1/T_2^R$) at high field. The analysis of the ^1H nuclear magnetic relaxation dispersion (^1H NMRD), that is given by the proton relaxivity measurements at different magnetic fields, can provide access to rotational correlation time (τ_R).

The $^{17}O–1/T_2^R$ profile as a function of the temperature of a 14.5 mM GdL^1 solution was recorded at 11.7 T and pH 7. The result is plotted in Figure 6 with the corresponding calculated curves for GdPCTA and GdDOTA at 7.05 T. The reduced ^{17}O transverse relaxation rates of GdL^1 show a continuous increase with decreasing temperature, indicating a maximum at temperature lower than 280 K and characteristic of a complex in the fast exchange regime. By comparison, the data obtained for GdPCTA show that its exchange rate in the investigated temperature range is in the fast to intermediate regime with a maximum around 290 K. These profiles markedly differ from that of GdDOTA which exhibits a classical bell shaped curve with a maximum around 308 K. A qualitative analysis of these data indicates that water exchange rate increases in the order GdDOTA < GdPCTA < GdL^1. Athough the number of data points is small, a theoretical treatment of the experimental data was attempted as previously described.[40] In the fit, the following parameters have been adjusted: the enthalpy and entropy of activation of the water-exchange process ($\Delta H^{\neq}$ and $\Delta S^{\neq}$), and the parameters describing electron spin relaxation ($B = 2.4\Delta^2$ and τ_V). The number of inner-sphere water molecule was fixed to $q = 2$, while the scalar coupling constant ($A/\hbar$) and the activation energy related to τ_v (E_v) were set to - 3.0×10^6 rad s^{-1} and 1 KJ mol^{-1}, respectively. The parameters resulting from the best fit are presented in Table 2. The large activation enthalpy ($\Delta H^{\neq}$) and the positive activation entropy ($\Delta S^{\neq}$) indicate that GdL^1 likely undergoes a dissociatively activated water exchange involving an eight-coordinate complex in the transition state.[41] This was also supported by the nine-coordinate ground state structure of this

View Article Online
DOI: 10.1039/C7DT00291B

complex. The water residence time was calculated at 298 and 310K, providing τ_M^{298} = 9.0 ± 0.6 ns and τ_M^{310} = 3.1 ± 0.2 ns values. The τ_M value of 9.0 ns is around 8 and 18 times shorter than those reported at 298 K for electrically neutral complexes GdPCTA (70 ns) and GdDO3A (160 ns).[42] These data show again that the introduction of an aromatic unit which rigidifies a ligand framework does not have a detrimental effect on the flexibility of the inner-sphere to limit water exchange and that complexes with negative overall charge have faster water exchange than neutral complexes. The faster water-exchange rate of GdL^1 relative to GdPCTA is also possibly due to the steric constraints at the site of water-coordination caused by the six-membered chelate ring formed after coordination of the phenolate to the metal ion in GdL^1 relative to the corresponding five-membered chelate ring in GdPCTA. The impact of expanding the chelate ring size in this way on τ_M is well documented. For example, a structural analogue of GdDOTA bearing an extra methylene carbon on the macrocyclic backbone (GdTRITA) displays a 66-fold shorter residence time compared to GdDOTA.[43] A shortening of τ_M was also observed by replacing a pyridyl donor by a pyridine *N*-oxide or a phenolate donor in one pendant arm of DO3A derivatives.[44] Interestingly, this τ_M value of 9 ns is also shorter than the values measured for other di-aqua complexes that lie in the range from 19 (Gd(TAM-TRI)) to 303 ns (Gd(PTDITA)).[36] The occurrence that τ_M does not limit the relaxation rate is also inferred from the qualitative analysis of the temperature dependence of r_1 at pH 7 and 20 MHz (Fig. 7). The complex exhibits an exponential increase in r_1 when the temperature is lowered from 318 to 278 K. This behaviour is quite typical for Gd chelates whose relaxivity is not limited by the coordinated water residence time but is largely dominated by rotational dynamics.

The ^{1}H NMRD profile of GdL^1 was determined at 310 K in the proton Larmor frequency range 15 kHz and 60 MHZ and was reported in Figure 8. This profile displays the typical s-shape of small size Gd^{III} chelates. It is characterized by two regions of constant r_1 with higher and lower relaxivity at low and high magnetic fields, respectively, and a single dispersion between 3 and 60 MHz. The possibility of self-aggregation was excluded by recording the ^{1}H NMRD profile for two different concentrations (0.90 and 1.81 mM), revealing an identical profile (See ESI, Fig. S13†). As we can see in Figure 8, the ^{1}H NMRD profiles of GdL^1 and its parent complex GdPCTA are quite similar, with only relaxivities at low field slightly higher for GdPCTA. This demonstrates again that a variation of the τ_M value has no effect on the relaxivity observed at 310 K for small-sized complexes if τ_M is smaller than 500 ns. The NMRD profile of GdL^1 was analyzed by a fitting procedure according to the established

View Article Online
DOI: 10.1039/C7DT00291B

theory for paramagnetic relaxation using the contributions from the inner-sphere and outer-sphere water molecules to the proton relaxivity (Solomon-Bloembergen-Morgan and Freed theories, respectively).[45] In this analysis, we have not taken into account the contribution of water molecules in the second coordination sphere, that is when these molecules are bound to the ligand. For the majority of polyaminocarboxylate complexes, the water molecules are not hydrogen bonded to the carboxylate oxygen atoms, in contrast with ligands bearing phosphorous acid functions.[46] In the fitting procedure, some parameters were fixed in agreement with previous studies: the metal-water proton distances in the first coordination sphere (r) and in the outer sphere (d) were fixed at 0.31 and 0.36 nm, respectively; the relative diffusion constant (D) was set at 3300 $\mu m^2\ s^{-1}$; τ_M was fixed at the value determined by ^{17}O relaxometry.[47] A good fit for the ^1H NMRD profile has been obtained with these fixed parameters (Fig. 8) and the most relevant parameters obtained are given in Table 3, together with analogous data of other relevant Gd^{III} complexes for comparison. The fitted value of τ_R (53 ps) is close to the values of structurally similar complexes reported in table 3, confirming that the complex does not self-assemble in the investigated concentration range.

An informative comparison is GdL^1 versus the commercially available mono-aqua GdDOTA with regard to the factors influencing the relaxometric properties. These two complexes share structural parameters, such as a 12-membered macrocyclic backbone and several bidentate aminoacetate chelating moieties and an overall negative charge. Besides, they differ from one another in the ligand denticity (heptadentate for H_4L^1 versus octadentate for H_4DOTA) and the presence of an aromatic unit concerning GdL^1. At 310 K and 20 or 60 MHz, the relaxivity of GdL^1 is 1.6 times higher than that of GdDOTA. The ^1H NMR profiles of the two complexes (Fig. 8) display the typical s-shape of low-molecular weight and rapidly tumbling chelates. Compared to GdDOTA, the profile of GdL^1 shows increased r_1 values over the entire investigated magnetic range. The difference in relaxivity is attenuated in the low magnetic field region, as a consequence of the higher value of the electronic relaxation time at zero field (τ_{SO}) for GdDOTA. This may be related to a higher symmetry of this complex with respect to GdL^1. As the two complexes have identical τ_R values (53 ps at 310 K) in agreement with the similar molecular weight of the ligands (MW = 409.4 and 404.4 g mol^{-1} for H_4L^1 and H_4DOTA, respectively), one concludes that the difference in the relaxivity is due to the hydration number differing by one unit. Besides, we notice a significant acceleration of the water exchange on the GdL^1 complex; at 298 K the $[GdL^1(H_2O)_2]^-$ species exchanges 27 times faster than $[GdDOTA(H_2O)]^-$ (39 times faster at 310 K). It is generally accepted that a

View Article Online
DOI: 10.1039/C7DT00291B

decrease of the residence time of the coordinated water molecule can be caused by several main factors: (i) a change in the mechanism of water exchange from a dissociatively activated process to an associatively activated process, (ii) a change in the overall charge of the complexes with more negative charge leading to faster exchange, (iii) an increased hindrance of the water coordination site.[48] The calculated values of the activation enthalpy and entropy of GdL^1 and GdDOTA[35a] ($\Delta H^{\neq}$ = 65.5 and 50.1 kJ mol^{-1}, $\Delta S^{\neq}$ = 129 and 48.7 J mol^{-1} K^{-1}, respectively) point to a dissociative activation mode of the water exchange mechanism in both complexes. The two complexes also display each a single negative overall charge and a similar charge density near the Gd^{III} ion. The introduction of a rigid aromatic unit and two six-membered chelate rings producing steric strains at the water binding sites may be identified as the two factors contributing to the acceleration of the water exchange. As a matter of fact, the leaving of the coordinated water molecule, which is the rate-determining step for a dissociatively activated water exchange, is largely facilitated by an increased steric crowding around the water molecule.[48]

Finally, GdL^1 satisfies the accepted empirical assay for kinetic stability (inertness) of Gd^{III} chelates, developed by Muller and coll. and applied by other research groups.[49,50] In this fast initial screening carried out close to physiological pH, Gd^{III} chelate was challenged in a phosphate-buffered solution with an equivalent concentration of Zn^{2+} ions (the most abundant endogenous metal ions with a concentration of ~ 32 μM in human plasma) and the occurrence of transmetallation was monitored by relaxometry. The procedure is based on the very low solubility of free Gd^{III} ions in phosphate solution (formation of $GdPO_4$ species with $K_{sp} = 10^{-22.2}$) and on the subsequent decrease of the relaxation rate R_1^p of the solution. In Figure 9, the evolution with time of the ratio of relaxation rates $R_1^p(t)/ R_1^p(t_0)$, where $R_1^p(t)$ and $R_1^p(t_0)$ are the relaxation rates at time t and zero, respectively, is shown for GdL^1 (2.5 mM) in phosphate buffer (67 mM, pH 7) in the absence or in the presence of Zn^{2+} ions (2.5 mM). No significant changes in relaxivity over a long period were observed for sample containing this Gd chelate after addition of 27 equiv of phosphate. This excludes a dissociation process or the formation of ternary complex with this anion, strengthening the results obtained by luminescence experiments with TbL^1. We can note that significant (~ 25 to 75%) effects of phosphate on the relaxivity of acyclic Gd^{III} complexes with two inner-sphere water molecules have been observed.[51] In the presence of Zn^{2+}, the relaxation rate R_1^p drops very slightly (7%) in the beginning of the experiment and then remains constant at least over a seven-day period. It can be concluded that the macrocyclic structure of GdL^1 is more kinetically inert than the acyclic structure GdDTPA and is as inert as macrocyclic complexes GdDO3A and GdPCTA.[35a,37, 50d]

View Article Online
DOI: 10.1039/C7DT00291B

Conclusions

This report describes new members of the class of polyaminocarboxylate macrocycles targeted for Ln^{III} complexation in aqueous solutions and whose Ln^{III} complexes may act as luminophores or paramagnetic contrastophores. The 12-membered (H_4L^1) and 24-membered (H_8L^2) macrocyclic ligands form hydrolytically stable mononuclear ($[(L^1)Ln(H_2O)_2]Na$) and dinuclear ($[(L^2)Ln_2)]Na_2$) complexes with the investigated lanthanide ions (Ln = Eu, Tb, Gd). The Tb^{III} complexes display efficient phenol-sensitized emission in the visible region (η_{sens} ~50%) with long emission lifetimes at room temperature (in the ms range) and high quantum yields (~ 50% in D_2O). The solution structure of $[(L^1)Tb(H_2O)_2]^-$, coupled with the occurrence of a residual negative charge, does not allow the replacement of the inner-sphere water molecules with bidentate anions such as carbonate, citrate or phosphate, as commonly observed for DO3A-based heptadentate complexes. At 20 MHz, the proton longitudinal relaxivities, r_1, of ($[(L^1)Gd(H_2O)_2]^-$) complex are 7.2 and 5.7 s^{-1} mM^{-1} (20 MHz, 298 and 310 K, respectively) and the rotational correlation time, τ_R, is 53 ps (310 K). These r_1 and τ_R values are comparable to those of Gd complexes with two water molecules in their first coordination sphere and similar molecular weight. Besides, the very short residence time of the coordinated water molecules (τ_M^{298K} = 9 ns) is in the range of the optimal values required for the attainment of very high relaxivity once the chelate would have been bound to a slowly rotating macromolecular structure. Moreover this complex is as stable in respect to transmetallation by Zn^{2+} ions as those with other macrocyclic ligands like DOTA or PCTA. The introduction of a phenolic ring instead of a pyridine ring in the 12-membered macrocyclic polyaminocarboxylate skeleton gives rise to; i) an excitation at lower energy ($\Delta\lambda$ ~ 30 nm) and a twofold increase of the luminescence brightness at λ_{max} due to a better sensitization efficiency (Tb complex) and ii) a higher water exchange rate of one order of magnitude between inner-sphere water molecules and bulk water due to the presence of a six-membered chelate ring in the coordination polyhedron (Gd complex). Finally, judicious substitution of the phenol unit should enable improved properties for luminescence and relaxometry of Ln^{III} complexes derived from this new family of polyaminocarboxylate macrocycles.

Experimental

View Article Online
DOI: 10.1039/C7DT00291B

General

^{1}H and ^{13}C spectra were recorded using a Bruker Avance 300 spectrometer operating at 300 MHz for ^{1}H and 75 MHz for ^{13}C or on a Bruker Avance 500 spectrometer operating at 500 MHz for ^{1}H and 125 MHz for ^{13}C. Chemical shifts are reported in ppm, with residual protonated solvents as the internal references. 2D DOSY ^{1}H NMR spectrum was recorded with a bipolar pulse pairs-stimulated echo pulse sequence with longitudinal eddy current delay[52] on the Bruker Avance 500 spectrometer equipped with a 5 mm cryoprobe at 298K (refer to ESI†). IR spectra were recorded on a Perkin-Elmer FT-IR 1725x spectrometer. Electrospray (ES) mass spectra were obtained on a Q TRAP Applied Biosystems spectrometer and High-Resolution Mass Spectra (HRMS) on a Xevo G2 QTof Waters spectrometer. Elemental analyses were recorded on a Perkin Elmer 2400 series II Simultaneous CHN elemental analyser at the "Service d'Analyse", Laboratoire de Chimie de Coordination (Toulouse). The analytical HILIC-UPLC analyses were performed on a Waters UPLC Acquity apparatus with PDA (photodiode array) and SQ (simple quadripole) detectors, and using an Acquity BEH HILIC column (1.7 μm, 100 × 2.1 mm) with a flow rate of 0.4 mL min^{-1}. Analyses were performed using a linear gradient system solvent A/solvent B 5/95 to 50/50 in 7 min, then an isocratic elution (50/50) for 10 min. For system 1, solvents were H_2O + 0.1% HCOOH (solvent A) and CH_3CN + 0.1% HCOOH (solvent B) and for system 2, solvents were ammonium formate buffer 10 mM pH8 (solvent A) and ammonium formate buffer 100 mM pH8/CH_3CN 10/90 (solvent B).

Photophysical experiments

Absorption measurements were done with a Hewlett Packard 8453 temperature-controlled spectrometer in 10 mm quartz cuvette. Emission, excitation spectra and luminescence decays at room temperature of lanthanide complexes were measured using a Cary Eclipse spectrofluorimeter equipped with a Xenon flash lamp source and a Hamamatsu R928 photomultiplier. At liquid-nitrogen temperature, a LS-50B Perkin-Elmer spectrofluorimeter equipped with a Xenon flash lamp source, a Hamamatsu R928 photomultiplier and the low-temperature accessory n° L2250136 was used. Excitation spectra were corrected for the excitation light intensity, while emission spectra were corrected for the instrument response.

Lifetimes τ (uncertainty $\leq$ 5%) are made by monitoring the decay at a wavelength corresponding to the maximum intensity of the emission spectrum, following pulsed excitation. They are the average values from at least five separate measurements covering two

View Article Online
DOI: 10.1039/C7DT00291B

or more lifetimes. The luminescence decay curves were fitted by an equation of the form $I(t) = I(0) \exp(-t/\tau)$ by using a curve-fitting program. The inner-sphere water coordination number (q) was calculated using equation: $q = A\ (k_H - k_D - k_{corr})$[18] where A is an empirically determined proportionality factor (A^{Eu} = 1.2 ms and A^{Tb} = 5.0 ms), k_H and k_D are the decay rate constants ($k = 1/\tau_{obs}$, τ_{obs} in ms) in H_2O and D_2O solutions respectively, and k_{corr} is a factor to correct for closely diffusing second-sphere water molecules (0.25 ms^{-1} and 0.06 ms^{-1} for Eu^{3+} and Tb^{3+}, respectively).

Quantum yields were determined by a comparative method with a standard reference; estimated experimental errors for quantum yield determination are ± 10%. Quinine sulfate in 1 N sulfuric acid (Φ = 0.546)[53] and $Cs_3[Tb(pic)_3]$ (Φ = 22 % in TRIS buffer pH 7.4)[54] were used as standards for Tb complexes and $[Ru(bpy)_3]Cl_2$ (Φ = 4% in water)[55] for Eu complexes.

Relaxometric experiments

In these experiments, the exact Gd^{III} concentration of solutions was determined by proton relaxivity measurements at 0.47 T and 37°C after mineralization in concentrated HNO_3.

The ^{17}O transverse relaxation times were measured using the standard Carr-Purcell-Meiboom-Gill spin-echo pulse sequence on 0.4 mL samples contained in 5 mm o.d. tubes on a Bruker Avance 500 spectrometer. The temperature was regulated by air or nitrogen flow controlled by a Bruker BVT 3200 unit. The value of q was obtained by comparing the O-17 chemical shifts measured at 330 K and 11.7 T (Bruker Avance-500 spectrometer) on solutions of Gd-DOTA (8.75 mM) and GdL^1 complex (9.5 mM) dissolved in 0.35 mL of water added 0.05 mL of D_2O for the lock.

Proton nuclear magnetic relaxation dispersion (NMRD) profiles were recorded over a magnetic field range from 0.015 to 40 MHz on a Stelar Spinmaster FFC fast field cycling NMR relaxometer. Measurements were performed at 310 K on 0.6 mL of solutions contained in 10 mm o.d. Pyrex tubes. Additional relaxation rates at 20 and 60 MHz were obtained on a Bruker Minispec mq20 and a Bruker Minispec mq60, respectively.

Transmetallation by Zn^{II} ions was evaluated from the decrease in the water proton longitudinal relaxation at 310 K and 20 MHz (Minispec mq20) of buffered solutions (pH 7, phosphate buffer: $[KH_2PO_4]$ = 26 mM, $[Na_2HPO_4]$ = 41 mM) containing the Gd^{III} complex (2.5 mM) and $ZnCl_2$ (2.5 mM).

View Article Online
DOI: 10.1039/C7DT00291B

N,N',N''-[(*tert*-Butoxycarbonyl)methyl]diethylenetriamine (1): This compound was synthesized following our procedure.[13]

2,6-bis(bromomethyl)-4-methylphenol (2): This compound was synthesized following a modified literature procedure.[56] At room temperature, a solution of 33% HBr in acetic acid (4 mL) was added to 2,6-bis(hydroxymethyl)-4-phenol (841 mg, 5 mmol). Upon stirring for 0.25 h, a sticky mass was formed and H_2O was added (10 mL). The mixture was stirred for an additional 0.5 h, and then filtered. The light yellow solid was sublimated under vacuum to give the product as a white solid (1.05 g, 71%). Mp: 116-118 °C. R_f (silicagel, CH_2Cl_2 /petroleum ether 40:60): 0.48. IR (KBr disc) ν/cm^{-1} 3519, 2915, 2839, 1603, 1486, 1210. ^{1}H NMR (300 MHz; $CDCl_3$): δ 2.26 (s, 3H), 4.54 (s, 4H), 5.44 (s, 1H), 7.08 (s, 2H). ^{13}C NMR (75 MHz; $CDCl_3$): δ 20.3 (CH_3), 29.5 (CH_2), 125.0 (Cq), 130.7 (Cq), 131.9 (CH), 151.0 (Cq). DCI-NH_3^+/MS: *m/z* 296.9, 294.9, 292.9 ($[M+H]^+$), 215.0, 213.0 ($[C_9H_{10}BrO]^+$).

Fully protected ligands 3 and 4

To a solution of triamine **1** (390 mg, 0.875 mmol) in dry acetonitrile (440 mL), was added in one portion sodium carbonate (0.93 g, 8.77 mmol) and then dibromo compound **2** (258 mg, 0.877 mmol). The suspension was heated at reflux for 16 h and was cooled to room temperature. The salts were filtered off and the filtrate was concentrated *in vacuo*. The oily residue was purified by chromatography on alumina eluting first with CH_2Cl_2, then with CH_2Cl_2/methanol (98:02) to give the expected macrocycles **3** (155 mg, 31%) and **4** (280 mg, 55%) as yellow oils.

By using similar reaction conditions but with Li_2CO_3 instead of Na_2CO_3 as base, macrocycles **3** and **4** were isolated in 63 and 23 yields, respectively.

Compound 3: R_f (alumina, CH_2Cl_2): 0.35. IR ν/cm^{-1} 2977, 2932, 2841, 1734, 1367, 1155. ^{1}H NMR (300 MHz; $CDCl_3$): δ 1.41 (s, 9H), 1.50 (s, 18H), 2.03-2.14 (m, 2H), 2.23 (s, 3H), 2.35-2.49 (m, 2H), 2.68-2.92 (m, 4H), 3.05 (s, 2H), 3.28 (d, J = 16.8 Hz, A part of an AB system, 2H), 3.35 (d, J = 16.8 Hz, B part of an AB system, 2H), 3.47 (d, J = 12.9 Hz, A part of an AX system, 2H), 4.32 (d, J = 12.9 Hz, X part of an AX system, 2H), 6.81 (s, 2H), 9.81 (s br, 1H). ^{13}C NMR (75 MHz; $CDCl_3$): δ 20.5 (CH_3), 28.1 (CH_3), 49.7 (CH_2), 51.0 (CH_2), 51.1 (CH_2), 55.7 (CH_2), 56.5 (CH_2), 80.6 (Cq), 81.2 (Cq), 125.8 (Cq), 128.2 (Cq), 130.4 (CH), 154.1 (Cq), 170.2 (CO), 170.3 (CO). ES$^+$/MS: *m/z* 578.4 ($[M+H]^+$, 100%).

View Article Online
DOI: 10.1039/C7DT00291B

Compound 4: R_f (alumina, CH_2Cl_2): 0.07. IR ν/cm^{-1} 2977, 2933, 2858, 1732, 1481, 1367, 1156. ^{1}H NMR (300 MHz; $CDCl_3$): δ 1.42 (s, 18H), 1.45 (s, 36H), 2.18 (s, 6H), 2.73-2.78 (m, 16H), 3.23 (s, 8H), 3.30 (s, 4H), 3.71 (s, 8H), 6.82 (s, 4H). ^{13}C NMR (75 MHz; $CDCl_3$): δ 20.4 (CH_3), 28.1 (CH_3), 51.3 (CH_2), 51.4 (CH_2), 53.8 (CH_2), 55.3 (CH_2), 55.4 (CH_2), 80.6 (Cq), 80.8 (Cq), 123.2 (Cq), 127.0 (Cq), 129.8 (CH), 153.7 (Cq), 170.5 (CO), 170.8 (CO). ES$^+$/MS: *m/z* 1157.7 ([M+H]$^+$, 100%), 578.4 ([M+2H]$^{2+}$, 47%).

Ligand H_4L^1: The triester **3** (100 mg, 0.173 mM) was stirred in a mixture of CH_2Cl_2 (5 mL) and HCl 20% in water (5 mL) at room temperature for 1 day. The aqueous layer was evaporated under reduced pressure to give H_4L^1 in the form of its hydrochloride salt as a beige powder (85 mg, 92%). UPLC analysis (system 1); t_R = 1.87 min. ^{1}H NMR (500 MHz; D_2O): δ 1.62-1.98 (m, 2H), 2.24 (s, 3H), 2.37-2.69 (m, 2H), 3.11-3.47 (m, 6H), 4.14 (s, 4H), 4.23 (d, J = 13.4 Hz, 2H), 4.98 (d, J = 13.4 Hz, 2H), 7.28 (s, 2H). ^{13}C NMR (125 MHz; D_2O): δ 19.4 (CH_3), 52.4 (CH_2), 53.7 (CH_2), 54.7 (CH_2), 57.4 (CH_2), 58.5 (CH_2), 122.7 (Cq), 133.6 (Cq), 134.7 (CH), 150.7 (Cq), 168.8 (CO), 175.0 (CO). ES$^+$/MS: *m/z* 410.1 ([M+H]$^+$, 100%). ES$^+$/HRMS Calcd for $C_{19}H_{28}N_3O_7$ [M+H]$^+$: *m/z* = 410.1927, found: *m/z* = 410.1915. Anal. Found: C, 42.30; H, 5.69; N, 7.45. Calcd for $C_{19}H_{27}N_3O_7$+3HCl+1H_2O: C, 42.51; H, 6.01; N, 7.83. UV/Vis λ_{max} (50 mM Tris buffer, pH 7.4)/nm: 229 sh (ε/dm^3 mol^{-1} cm^{-1} 5990), 288 (2490).

Ligand H_8L^2:

The hexaester **4** (100 mg, 0.087 mM) was stirred in a mixture of CH_2Cl_2 (5 mL) and HCl 20% in water (5 mL) at room temperature for 1 day. The aqueous layer was evaporated under reduced pressure to give H_8L^2 in the form of its hydrochloride salt as a beige powder (81 mg, 85%). UPLC analysis (system 2); t_R = 4.47 min. ^{1}H NMR (300 MHz; $CDCl_3$): δ 2.18 (s, 6H), 2.92-3.11 (m, 8H), 3.21 (s, 4H), 3.26-3.44 (m, 8H), 3.76 (s, 8H), 4.33 (s, 8H), 7.21 (s, 4H). ^{13}C NMR (75 MHz; D_2O): δ 19.3 (CH_3), 49.0 (CH_2), 52.1 (CH_2), 53.9 (CH_2), 55.3 (CH_2), 55.6 (CH_2), 118.4 (Cq), 131.6 (Cq), 135.7 (CH), 152.9 (Cq), 170.2 (CO), 174.2 (CO). ES$^+$/MS: *m/z* 841.3 ([M+Na]$^+$, 100%), 819.3 ([M+H]$^+$, 35%). ES$^+$/HRMS Calcd for $C_{38}H_{54}N_6O_{14}Na$ [M+Na]$^+$: *m/z* = 841.3596, found: *m/z* = 841.3657; calcd for $C_{38}H_{55}N_6O_{14}$ [M+H]$^+$: *m/z* = 819.3776, found: *m/z* = 819.3807. Anal. Found: C, 42.13; H, 6.13; N, 7.53. Calcd for $C_{38}H_{54}N_6O_{14}$+6HCl+3H_2O: C, 41.81; H, 6.09; N, 7.70. UV/Vis λ_{max} (50 mM Tris buffer, pH 7.4)/nm: 224 sh (ε/dm^3 mol^{-1} cm^{-1} 15120), 288 (6510).

View Article Online
DOI: 10.1039/C7DT00291B

[LnL^1]Na and [Ln$_2$L^2]Na$_2$ complexes. General procedure: To a solution of ligand in H_2O was added $LnCl_3$,6H_2O (1.1 equiv.). After stirring at room temperature for 1h, pH was adjusted to 5-6 with NaOH 0.1 M and the mixture was then stirred overnight at room temperature. The pH was then adjusted to 7 with NaOH 0.1 M, the solvent was evaporated to a minimum and the solution was loaded on a Waters Sep-Pak® cartridge (C_{18}, 10 g). Cartridge was rinsed with H_2O to remove salts and the product was eluted with a H_2O/MeOH 1:1 mixture. The solvents were removed *in vacuo* to give the expected complexes with quantitative yields. The absence of free Ln^{III} ions in these complexes was verified using a classic test with an arsenazo indicator solution.

[TbL^1]Na: UPLC analysis (system 1); t_R = 3.43 min. ES$^-$/HRMS Calcd for $C_{19}H_{23}N_3O_7Tb$ $[TbL^1]^-$: m/z = 564.0789, found: m/z = 564.0800. UV/Vis λ_{max} (50 mM Tris buffer, pH 7.4)/nm: 245 (ε/dm^3 mol^{-1} cm^{-1} 6480), 296 (2980). Luminescence λ_{em} (50 mM Tris buffer, pH 7.4; 298 K; λ_{exc} = 296 nm)/nm: 490 (relative intensity, corrected spectrum 35), 545 (100), 586 (26), 623 (15), 638-700 (6).

[EuL^1]Na: UPLC analysis (system 1); t_R = 3.46 min. ES$^-$/HRMS Calcd for $C_{19}H_{23}N_3O_7Eu$ $[EuL^1]^-$: m/z = 558.0748 (^{153}Eu) and 556.0734 (^{151}Eu), found: m/z = 558.0756 and m/z = 556.0742, respectively. UV/Vis λ_{max} (50 mM Tris buffer, pH 7.4)/nm: 245 (ε/dm^3 mol^{-1} cm^{-1} 7680), 296 (3650). Luminescence λ_{em} (50 mM Tris buffer, pH 7.4; 298 K; λ_{exc} = 296 nm)/nm: 592 (relative intensity, corrected spectrum 32), 616 (100), 652 (4), 698 (65).

[GdL^1]Na:UPLC analysis (system 1); t_R = 3.47 min. ES$^-$/HRMS Calcd for $C_{19}H_{23}N_3O_7Gd$ $[GdL^1]^-$: m/z = 563.0782 (^{158}Gd), found: m/z = 563.0778. UV/Vis λ_{max} (50 mM Tris buffer, pH 7.4)/nm: 245 (ε/dm^3 mol^{-1} cm^{-1} 5960), 296 (2810). Fluorescence λ_{em} (50 mM Tris buffer, pH 7.4; 298 K; λ_{exc} = 296 nm)/nm: 338. Phosphorescence λ_{em} (50 mM Tris buffer/glycerol 4:1; 77 K; λ_{exc} = 296 nm)/nm: 405; lifetime 1.48 ms.

[Tb$_2$L^2]Na$_2$: UPLC analysis (system 2); t_R = 3.88 min. ES$^-$/HRMS Calcd for $C_{38}H_{47}N_6O_{14}Tb_2$ $[Tb_2L^2+H]^-$: m/z = 1129.1658, found: m/z = 1129.1636; calcd for $C_{38}H_{46}N_6O_{14}Tb_2$ $[Tb_2L^2]^{2-}$: m/z = 564.0789, found: m/z = 564.0796. UV/Vis λ_{max} (50 mM Tris buffer, pH 7.4)/nm: 242 (ε/dm^3 mol^{-1} cm^{-1} 16850), 296 (6920). Luminescence λ_{em} (50 mM Tris buffer, pH 7.4; 298 K; λ_{exc} = 296 nm)/nm: 490 (relative intensity, corrected spectrum 37), 545 (100), 585 (27), 622 (15), 638-700 (7).

[Eu$_2$L^2]Na$_2$: UPLC analysis (system 2); t_R = 4.09 min. ES$^-$/MS: m/z 1137.2 ($[^{151,153}Eu_2L^2+Na]^-$, 100%), 1115.3 ($[^{151,153}Eu_2L^2+H]^-$, 27%), UV/Vis λ_{max} (50 mM Tris buffer, pH 7.4)/nm: 242 (ε/dm^3 mol^{-1} cm^{-1} 15250), 295 (6390). Luminescence λ_{em} (50 mM Tris buffer,

View Article Online
DOI: 10.1039/C7DT00291B

pH 7.4; 298 K; λ_{exc} = 296 nm)/nm: 593 (relative intensity, corrected spectrum 35), 617 (100), 652 (7), 697 (72).

$[Gd_2L^{2l}Na_2$: UPLC analysis (system 2); t_R = 4.05 min. ES^-/HRMS Calcd for $C_{38}H_{46}N_6O_{14}Gd_2Na$ $[Gd_2L^2+Na]^-$: m/z = 1149.1470 (^{158}Gd), found: m/z = 1149.1451; calcd for $C_{38}H_{47}N_6O_{14}Gd_2$ $[Gd_2L^2+H]^-$: m/z = 1127.1650 (^{158}Gd), found: m/z = 1127.1626; calcd for $C_{38}H_{46}N_6O_{14}Gd_2$ $[Gd_2L^2]^{2-}$: m/z = 563.0786 (^{158}Gd), found: m/z = 563.0791. UV/Vis λ_{max} (50 mM Tris buffer, pH 7.4)/nm: 242 (ε/dm^3 mol^{-1} cm^{-1} 15790), 296 (6740). Fluorescence λ_{em} (50 mM Tris buffer, pH 7.4; 298K; λ_{exc} = 296 nm)/nm: 329. Phosphorescence λ_{em} (50 mM Tris buffer/glycerol 4:1; 77 K; λ_{exc} = 296 nm)/nm: 416

Acknowledgements

We thank Isabelle Fabing for technical assistance on UPLC equipment provided by the Integrated Screening Platform of Toulouse (PICT, IBiSA). This work was supported by the French Ministère de la Recherche (Ph.D. grant for M.E.) and the CNRS. S.L. and L.V.E. thank the FNRS (*Fonds National de la recherche scientifique*), and ARC Programs (AUWB-2010-10/15-UMONS-5) of the French Community of Belgium, the UIAP VII program of Belgium and the Center for Microscopy and Molecular Imaging (CMMI, supported by the European Regional Development Fund and the Walloon Region).

References

1 (a) S. Goswami, S. Maity, A. C. Maity, A. Kumar Das, K. Khanra, T. Kanti Mandal and N. Bhattacharyya, *Tetrahedron Lett.*, 2014, **55**, 5993-5997; (b) K. Zhang, C. Jin, H.-Q. Chen, G. Yin and W. Huang, *Chem. Asian J.*, 2014, **9**, 2534-2541; (c) Y.-Y. Liu, W.-J. Gong, J.-C. Ma and J.-F. Ma, *J. Coord. Chem.*, 2013, **66**, 4032–4051; (d) Y. Fu, Z. Xing, C. Zhu, H. Yang, W. He, C. Zhu and Y. Cheng, *Tetrahedron Lett.*, 2012, **53**, 804-807;(e) G. Ambrosi, M. Formica, V. Fusi, L. Giorgi, E. Macedi, M. Micheloni and R. Pontellini, *Inorg. Chim. Acta*, 2009, **362**, 3709-3714; (f) G. Ambrosi, M. Formica, V. Fusi, L. Giorgi and M. Micheloni, *Coord. Chem. Rev.*, 2008, **252**, 1121-1152; (g) H. Okawa, H. Furutachi and D. E. Fenton, *Coord. Chem. Rev.*, 1998, **174**, 51-75.

View Article Online
DOI: 10.1039/C7DT00291B

2 (a) H. Nakai, T. Goto, K. Kitagawa, K. Nonaka, T. Matsumoto and S. Ogo, *Chem. Commun.*, 2014, **50**, 15737-15739; (b) H. Nakai, K. Nonaka, T. Goto, J. Seo, T. Matsumoto and S. Ogo, *Dalton Trans.*, 2015, **44**, 10923-10927; (c) B. Makhinson, A. K. Duncan, A. R. Elam, A. de Bettencourt-Dias, C. D. Medley, J. E. Smith and E. J. Werner, *Inorg. Chem.*, 2013, **52**, 6311-6318; (d) P. Gawryszewska and J. Lisowski, *Inorg. Chim. Acta*, 2012, **383**, 220-229.

3 M. Woods, G. E. Kiefer, S. Bott, A. Castillo-Muzquiz, C. Eshelbrenner, L. Michaudet, K. McMillan, S. D. K. Mudigunda, D. Ogrin, G. Tircso, S. Zhang, P. Zhao and A. D. Sherry, *J. Am. Chem. Soc.*, 2004, **126**, 9248-9256

4 O. A. Blackburn, M. Tropiano, L. S. Natrajan, A. M. Kenwright and S. Faulkner, *Chem. Commun.*, 2016, **52**, 6111-6114.

5 C. Platas, F. Avecilla, A. de Blas, T. Rodríguez-Blas, C. F. G. C. Geraldes, E. Toth, A. E. Merbach and J.-C. G. Bünzli, *J. Chem. Soc., Dalton Trans.*, 2000, 611-618.

6 (a) N. Leygue, A. Boulay, C. Galaup, E. Benoist, S. Laurent, L. Vander Elst, B. Mestre-Voegtle and C. Picard, *Dalton Trans.*, 2016, **45**, 8379-8393; (b) S. Laurent, L. Vander Elst, C. Galaup, N. Leygue, S. Boutry, C. Picard and R. N. Muller, *Contrast Media Mol. Imaging*, 2014, **9**, 300-312; (c) C. Picard, N. Geum, I. Nasso, B. Mestre, P. Tisnes, S. Laurent, R. N. Muller and L. Vander Elst, *Bioorg. Med. Chem. Lett.*, 2006, **16**, 5309-5312; (d) I. Nasso, C. Galaup, F. Havas, P. Tisnès, C. Picard, S. Laurent, L. Vander Elst and R. N. Muller, *Inorg. Chem.*, 2005, **44**, 8293-8305.

7 K. W.-Y. Chan and W.-T. Wong, *Coord. Chem. Rev.*, 2007, **251**, 2428-2451.

8 A. de Bettencourt-Dias, *Curr. Org. Chem.*, 2007, **11**, 1460-1480.

9 See for examples: (a) L. J. Charbonniere, S. Mameri, D. Flot, F. Waltz, C. Zandanel and R. F. Ziessel, *Dalton Trans.*, 2007, 2245-2253; (b) A. Nonat, P. H. Fries, J. Pécaut and M. Mazzanti, *Chem. Eur. J.*, 2007, **13**, 8489-8506.

10 N. Sabbatini, M. Guardigli and J.-M. Lehn, *Coord. Chem. Rev.*, 1993, **123**, 201-228.

View Article Online
DOI: 10.1039/C7DT00291B

11 L. S. Natrajan, P. L. Timmins, M. Lunn and S. L. Heath, *Inorg. Chem.*, 2007, **46**, 10877-10886.

12 (a) W. D. Kim, G. E. Kiefer, F. Maton, K. McMillan, R. N. Muller and A. D. Sherry, *Inorg. Chem.*, 1995, **34**, 2233-2243 ; (b) S. Aime, M. Botta, S. Geninatti Crich, G. B. Giovenzana, G. Jommi, R. Pagliarin and M. Sisti, *Inorg. Chem.*, 1997, **36**, 2992-3000 ; (c) J.-M. Siaugue, F. Segat-Dioury, A. Favre-Reguillon, V. Wintgens, C. Madic, J. Foos and A. Guy, *J. Photochem. Photobiol. A*, 2003, **156**, 23-29; (d) G. Tircso, Z. Kovacs and A. D. Sherry, *Inorg. Chem.*, 2006, **45**, 9269-9280.

13 C. Galaup, J.-M. Couchet, S. Bedel, P. Tisnès and C. Picard, *J. Org. Chem.*, 2005, **70**, 2274-2284.

14 (a) G. Ambrosi, M. Formica, V. Fusi, L. Giorgi, E. Macedi, M. Micheloni, P. Paoli and P. Rossi, *Inorg. Chem.*, 2009, **48**, 10424-10434; (b) H.-H. Chen, J. Yang, Y.-Y. Liu and J.-F. Ma, *CrystEngComm*, 2013, **15**, 5168-5178.

15 (a) L. Ma, L. Lu, M. Zhu, Q. Wang, F. Gao, C. Yuan, Y. Wu, S. Xing, X. Fu, Y. Mei and X. Gao, *J. Inorg. Biochem.*, 2011, **105**, 1138-1147; (b) J. Kankare, A. Karppi and H. Takalo, *Anal. Chim. Acta*, 1994, **295**, 27-35; (c) J. Kankare, K. Haapakka, S. Kulmala, V. Nanto, J. Eskola and H. Takalo, *Anal. Chim. Acta*, 1992, **266**, 205-212.

16 F. S. Richardson, *Chem. Rev.*, 1982, **82**, 541-552.

17 (a) W. D. W. Horrocks Jr. and D. R. Sudnick, *Acc. Chem. Res.*, 1981, **14**, 384-392; (b) W. D. W. Horrocks Jr. and D. R. Sudnick, *J. Am. Chem. Soc.*, 1979, **101**, 334-340.

18 A. Beeby, I. M. Clarkson, R. S. Dickins, S. Faulkner, D. Parker, L. Royle, A. S. de Sousa, J. A. G. Williams and M. Woods, *J. Chem. Soc., Perkin Trans. 2*, 1999, 493-503.

19 S. A. Cotton, *Comptes Rendus Chimie*, 2005, **8**, 129-145.

20 S. V. Eliseeva and J.-C. G. Bünzli, *Chem. Soc. Rev.*, 2010, **39**, 189-227.

View Article Online
DOI: 10.1039/C7DT00291B

21 O. N. Tchaikovskaya, I. V. Sokolova, R. T. Kuznetsova, V. A. Swetlitchnyi, T. N. Kopylova and G. V. Mayer, *J. Fluoresc*, 2000, **10**, 403-408.

22 T. Ala-Kleme, K. Haapakka and M. Latva, *Anal. Chim. Acta*, 1999, **395**, 205-211.

23 C. P. Montgomery, B. S. Murray, E. J. New, R. Pal and D. Parker, *Acc. Chem. Res.*, 2009, **42**, 925-937.

24 M. Latva, H. Takalo, V.-M. Mukkala, C. Matachescu, J.-C. Rodriguez-Ubis and J. Kankare, *J. Lumin.*, 1997, **75**, 149-169.

25 (a) M. Xiao and P. R. Selvin, *J. Am. Chem. Soc.*, 2001, **123**, 7067-7073; (b) J. Xu, T. M. Corneillie, E. G. Moore, G.-L. Law, N. G. Butlin and K. N. Raymond, *J. Am. Chem. Soc.*, 2011, **133**, 19900-19910.

26 E. Brunet, O. Juanes, R. Sedano and J.-C. Rodríguez-Ubis, *Org. Lett.*, 2002, **4**, 213-216.

27 See for examples: (a) A. P. Bassett, S. W. Magennis, P. B. Glover, D. J. Lewis, N. Spencer, S. Parsons, R. M. Williams, L. De Cola and Z. Pikramenou, *J. Am. Chem. Soc.*, 2004, **126**, 9413-9424; (b) P. Gawryszewska, J. Sokolnicki, A. Dossing, J. P. Riehl, G. Muller and J. Legendziewicz, *J. Phys. Chem. A*, 2005, **109**, 3858-3863; (c) I. Nasso, S. Bedel, C. Galaup and C. Picard, *Eur. J. Inorg. Chem.*, 2008, 2064-2074; (d) A. R. Ramya, M. L. P. Reddy, A. H. Cowley and K. V. Vasudevan, *Inorg. Chem.*, 2010, **49**, 2407-2415.

28 A. E. Martell, R. M. Smith, *Critical Stability Constants*, Plenum Press, New York, **1974**, vol.1, p 282.

29 See for examples: (a) J. I. Bruce, R. S. Dickins, L. J. Govenlock, T. Gunnlaugsson, S. Lopinski, M. P. Lowe, D. Parker, R. D. Peacock, J. J. B. Perry, S. Aime and M. Botta, *J. Am. Chem. Soc.*, 2000, **122**, 9674-9684; (b) V. C. Pierre, M. Botta, S. Aime and K. N. Raymond, *Inorg. Chem.*, 2006, **45**, 8355-8364; (c) D. Imperio, G. B. Giovenzana, G.-I. Law, D. Parker and J. W. Walton, *Dalton Trans.*, 2010, **39**, 9897-9903.

View Article Online
DOI: 10.1039/C7DT00291B

30 L. S. Nikolaeva, V. V. Chirkov, N. A. Dobrynina, L. A. Lyapina and V. E. Pastorova, *Pharm. Chem. J.*, 2005, **39**, 57-63.

31 G. Mathis, *Clin. Chem.*, 1993, **39**, 1953-1959.

32 L. R. Morss, *Chem. Rev.*, 1976, **76**, 827-841.

33 S. J. A. Pope, A. M. Kenwright, S. L. Heath and S. Faulkner, *Chem. Commun.*, 2003, 1550-1551.

34 C. Guanci, G. Giovenzana, L. Lattuada, C. Platas-Iglesias and L. J. Charbonniere, *Dalton Trans.*, 2015, **44**, 7654-7661.

35 (a) S. Laurent, L. Vander Elst and R. N. Muller, *Contrast Media Mol. Imaging*, 2006, **1**, 128–137; (b) D. H. Powell, O. M. Ni Dhubhghaill, D. Pubanz, L. Helm, Y. S. Lebedev, W. Schlaepfer and A. E. Merbach, *J. Am. Chem. Soc.*, 1996, **118**, 9333-9346.

36 (a) A. Vagner, E. Gianolio, S. Aime, A. Maiocchi, I. Toth, Z. Baranyai and L. Tei, *Chem. Commun.*, 2016, **52**, 11235-11238; (b) C. S. Bonnet, S. Laine, F. Buron, G. Tircso, A. Pallier, L. Helm, F. Suzenet and E. Toth, *Inorg. Chem.*, 2015, **54**, 5991-6003; (c) Z. Baranyai, L. Tei, G. B. Giovenzana, F. K. Kalman and M. Botta, *Inorg. Chem.*, 2012, **51**, 2597-2607; (d) C. S. Bonnet, F. Buron, F. Caillé, C. M. Shade, B. Drahos, L. Pellegatti, J. Zhang, S. Villette, L. Helm, C. Pichon, F. Suzenet, S. Petoud and E. Toth, *Chem. Eur. J.*, 2012, **18**, 1419-1431; (e) G. Tallec, D. Imbert, P. H. Fries and M. Mazzanti, *Dalton Trans.*, 2010, **39**, 9490-9492; (f) S. Aime, L. Calabi, C. Cavallotti, E. Gianolio, G. B. Giovenzana, P. Losi, A. Maiocchi, G. Palmisano and M. Sisti, *Inorg. Chem.*, 2004, **43**, 7588-7590; (g) M. K. Thompson, M. Botta, G. Nicolle, L. Helm, S. Aime, A. E. Merbach and K. N. Raymond, *J. Am. Chem. Soc.*, 2003, **125**, 14274-14275.

37 M. Port, I. Raynal, L. Vander Elst, R. N. Muller, F. Dioury, C. Ferroud and A. Guy, *Contrast Media Mol. Imaging*, 2006, **1**, 121-127.

38 P. Hermann, J. Kotek, V. Kubicek and I. Lukes, *Dalton Trans.*, 2008, 3027-3047.

View Article Online
DOI: 10.1039/C7DT00291B

39 P. Caravan, *Chem. Soc. Rev.*, 2006, **35**, 512-523.

40 (a) L. Vander Elst, F. Maton, S. Laurent, F. Seghi, F. Chapelle and R. N. Muller, *Magn. Reson. Med.*, 1997, **38**, 604-614; (b) R. N. Muller, B. Radüchel, S. Laurent, J. Platzek, C. Piérart, P. Mareski and L. Vander Elst, *Eur. J. Inorg. Chem.*, 1999, 1949-1955; (c) S. Laurent, L. Vander Elst, S. Houzé, N. Guérit and R. N. Muller, *Helv. Chim. Acta*, 2000, **83**, 394-406.

41 K. Micskei, L. Helm, E. Brucher and A. E. Merbach, *Inorg. Chem.*, 1993, **32**, 3844-3850.

42 S. Aime, M. Botta, S. Geninatti Crich, G. Giovenzana, R. Pagliarin, M. Sisti and E. Terreno, *Magn. Reson. Chem.*, 1998, **36**, S200-S208.

43 S. Laus, R. Ruloff, E. Toth and A. E. Merbach, *Chem. Eur. J.*, 2003, **9**, 3555-3566.

44 (a) M. Polasek, M. Sedinova, J. Kotek, L. Vander Elst, R. N. Muller, P. Hermann and I. Lukes, *Inorg. Chem.*, 2009, **48**, 455-465; (b) S. Dumas, V. Jacques, W.-C. Sun, J. S. Troughton, J. T. Welch, J. M. Chasse, H. Schmitt-Willich and P. Caravan, *Invest. Radiol.*, 2010, **45**, 600-612.

45 S. Laurent, C. Henoumont, L. Vander Elst and R. N. Muller, *Eur. J. Inorg. Chem.*, 2012, 1889-1915.

46 (a) S. Aime, E. Gianolio, D. Corpillo, C. Cavallotti, G. Palmisano, M. Sisti, G. B. Giovenzana and R. Pagliarin, *Helv. Chim. Acta*, 2003, **86**, 615-632 ; (b) S. Aime, M. Botta, L. Frullano, S. Geninatti Crich, G. Giovenzana, R. Pagliarin, G. Palmisano, F. Riccardi Sirtori and M. Sisti, *J. Med. Chem.*, 2000, **43**, 4017-4024.

47 L. Vander Elst, A. Sessoye, S. Laurent and R. N. Muller, *Helv. Chim. Acta*, 2005, **88**, 574-587.

48 a) A. S. Merbach, L. Helm and E. Toth, in *The Chemistry of Contrast Agents in Medical Magnetic Resonance Imaging*, 2nd edition, ed. A. S. Merbach, L. Helm and E. Toth, John Wiley & Sons, Chischester, 2013, chapter 2, 25-81; b) B. N. Siriwardena-Mahanama and M. J. Allen, *Molecules*, 2013, **18**, 9352-9381.

View Article Online
DOI: 10.1039/C7DT00291B

49 (a) S. Laurent, L. Vander Elst, F. Copoix and R. N. Muller, *Invest. Radiol.*, 2001, **36**, 115-122; (b) S. Laurent, L. Vander Elst, C. Henoumont and R. N. Muller, *Contrast Media Mol. Imaging*, 2010, **5**, 305-308.

50 (a) J. Yu, A. F. Martins, C. Preihs, V. Clavijo Jordan, S. Chirayil, P. Zhao, Y. Wu, K. Nasr, G. E. Kiefer and A. D. Sherry, *J. Am. Chem. Soc.*, 2015, **137**, 14173-14179; (b) M. Moula Karimdjy, G. Tallec, P. H. Fries, D. Imbert and M. Mazzanti, *Chem. Commun.*, 2015, **51**, 6836-6838; (c) A. C. Mendonça, A. F. Martins, A. Melchior, S. M. Marques, S. Chaves, S. Villette, S. Petoud, P. L. Zanonato, M. Tolazzi, C. S. Bonnet, E. Toth, P. Di Bernardo, C. F. G. C. Geraldes and M. A. Santos, *Dalton Trans.*, 2013, **42**, 6046-6057; (d) M. Polasek and P. Caravan, *Inorg. Chem.*, 2013, **52**, 4084-4096; (e) K.-H. Jung, H.-K. Kim, G. H. Lee, D.-S. Kang, J.-A. Park, K. M. Kim, Y. Chang and T.-J. Kim, *J. Med. Chem.*, 2011, **54**, 5385-5394; (f) L. Moriggi, C. Cannizzo, C. Prestinari, F. Berrière and L. Helm, *Inorg. Chem.*, 2008, **47**, 8357-8366.

51 (a) S. Silverio, S. Torres, A. F. Martins, J. A. Martins, J. P. André, L. Helm, M. I. M. Prata, A. C. Santos and C. F. G. C. Geraldes, *Dalton Trans.*, 2009, 4656-4670; J. B. Livramento, A. Sour, A. Borel, A. E. Merbach and E. Toth, *Chem. Eur. J.*, 2006, **12**, 989-1003.

52 C. S. Johnson Jr, *Prog Nucl Magn Reson Spectrosc.*, 1999, **34**, 203-256.

53 S. R. Meech and D. Phillips, *J. Photochem.*, 1983, **23**, 193-217.

54 (a) A.-S. Chauvin, F. Gumy, D. Imbert and J.-C. G. Bünzli, *Spectrosc. Lett.*, 2004, **37**, 517-532; (b) A.-S. Chauvin, F. Gumy, D. Imbert and J.-C. G. Bünzli, *Spectrosc. Lett.*, 2007, **40**, 193.

55 H. Ishida, S. Tobita, Y. Hasegawa, R. Katoh and K. Nozaki, *Coord. Chem. Rev.*, 2010, **254**, 2449-2458.

56 B. M. Trost, V. S. C. Yeh, H. Ito and N. Bremeyer, *Org. Lett.*, 2002, **4**, 2621-2623.

View Article Online
DOI: 10.1039/C7DT00291B

Captions

Fig. 1 Chemical structures of H_4L^1, H_8L^2 and other ligands discussed in this work.

Fig. 2 ^{1}H DOSY NMR spectrum (500 MHz, $CDCl_3$) of the crude mixture resulting from reaction between triamine **1** and dibromo compound **2**. ^{1}H NMR resonances of macrocycles **3** (closed circles) and **4** (open circles).

Fig. 3 Corrected emission spectra of TbL^1 and Tb_2L^2 complexes recorded at room temperature in Tris buffer (pH 7.4). The emission spectra resulted from a UV-light excitation at 296 nm. The insets show the total emission intensity of solutions of H_4L^1 or H_8L^2 as the function of $TbCl_3$ added in Tris buffer (pH 7.4).

Fig. 4 Schematic representation of mononuclear LnL^1, LnPCTA complexes and dinuclear Ln_2L^2 complexes.

Fig. 5 Normalized (a) absorption (- - -), (b) fluorescence (——) and (c) phosphorescence (-·-·-·-) spectra of GdL^1 and Gd_2L^2 complexes. The absorption and fluorescence spectra were measured at 298 K in Tris buffer (pH 7.4) and the phosphorescence spectra at 77 K in Tris buffer-glycerol (4:1 v/v) glassy matrix.

Fig. 6 Reduced transverse ^{17}O relaxation rate of water ($1/T_2^R$) for aqueous solutions of GdL^1 (closed circles) at 11.75 T, GdPCTA (open circles) and GdDOTA (closed triangles) at 7.05 T.[35a]

Fig. 7 Temperature (278 – 318 K) dependence of the proton longitudinal relaxivity, r_1, of GdL^1 complex in water at 20 MHz.

Fig. 8 Proton NMRD data obtained at 310 K on a 0.90 mM GdL^1 (closed circles), a 0.54 mM GdPCTA solution (open circles) and a 1.5 mM GdDOTA (closed triangles) solution in water. The lines correspond to the theoretical fittings.

Fig. 9 Evolution of the ratio $R_1^p(t)/R_1^p(t_0)$ (T = 310 K, B_0 = 0.47 T, 20 MHz) vs. time for solutions of GdL^1 in phosphate buffer (67 mM, pH 7.0) (open circles), GdL^1 (closed circles) and GdDTPA (dashed line) in phosphate buffer containing an equimolar amount of Zn^{2+} ions.

View Article Online
DOI: 10.1039/C7DT00291B

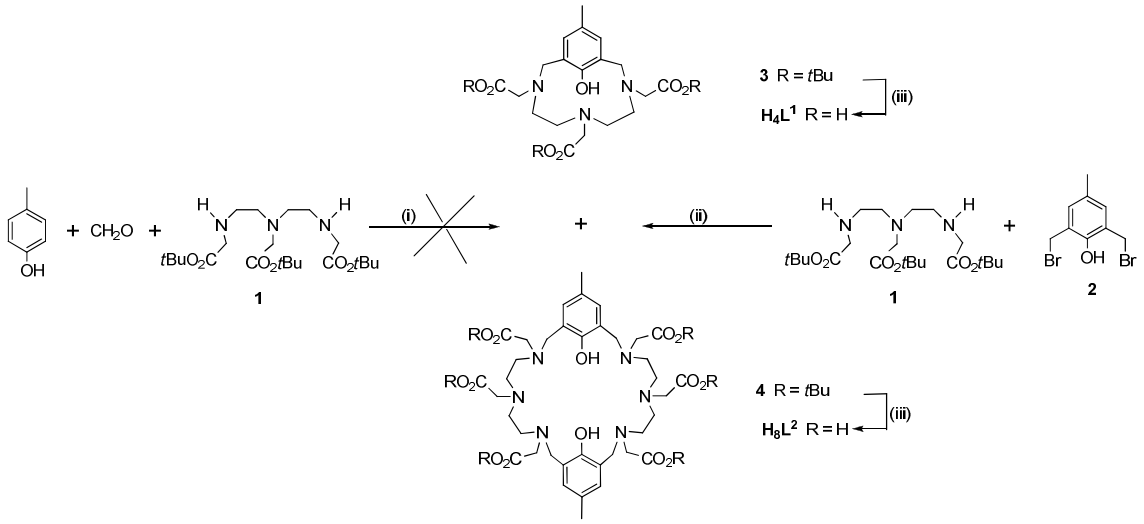

Scheme 1 Synthesis of ligands H_4L^1 and H_8L^2.

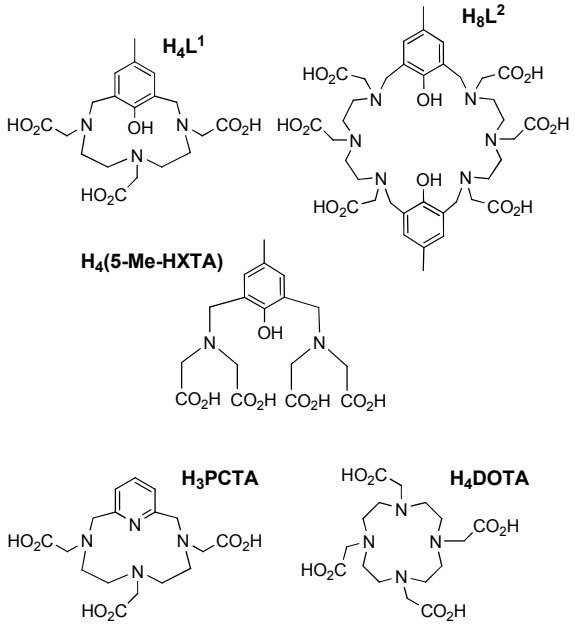

Fig. 1 Chemical structures of H_4L^1, H_8L^2 and other ligands discussed in this work.

View Article Online
DOI: 10.1039/C7DT00291B

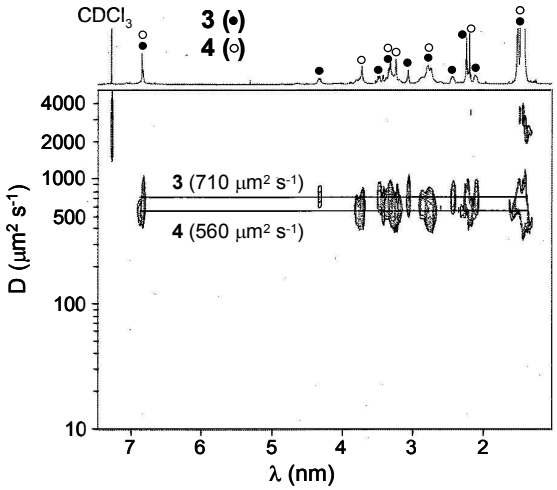

Fig. 2 ^{1}H DOSY NMR spectrum (500 MHz, $CDCl_3$) of the crude mixture resulting from reaction between triamine **1** and dibromo compound **2**. ^{1}H NMR resonances of macrocycles **3** (closed circles) and **4** (open circles).

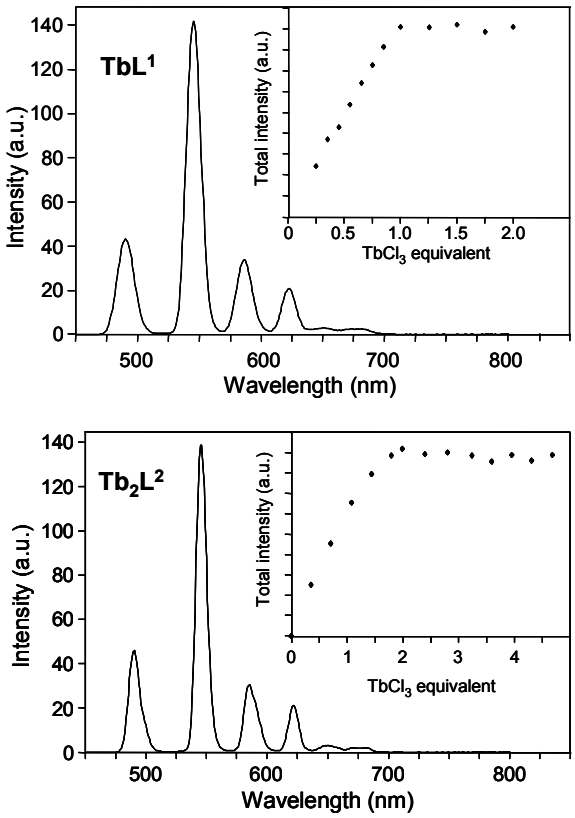

Fig. 3 Corrected emission spectra of TbL^1 and Tb_2L^2 complexes recorded at room temperature in Tris buffer (pH 7.4). The emission spectra resulted from a UV-light excitation at 296 nm. The insets show the total emission intensity of solutions of H_4L^1 or H_8L^2 as the function of $TbCl_3$ added in Tris buffer (pH 7.4).

View Article Online
DOI: 10.1039/C7DT00291B

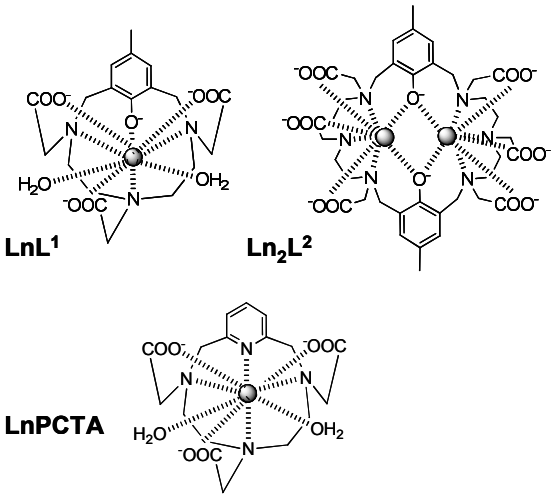

Fig. 4 Schematic representation of mononuclear LnL^1, LnPCTA complexes and dinuclear Ln_2L^2 complexes.

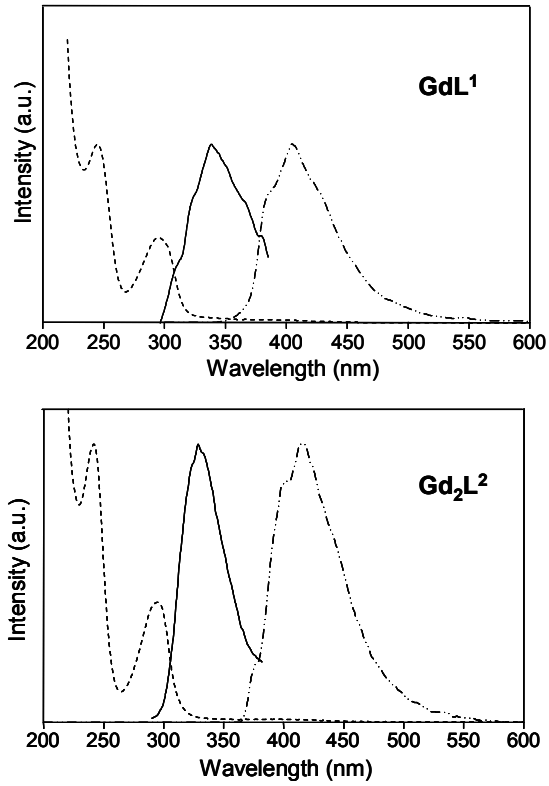

Fig. 5 Normalized (a) absorption (- - -), (b) fluorescence (——) and (c) phosphorescence (-·-·-·) spectra of GdL^1 and Gd_2L^2 complexes. The absorption and fluorescence spectra were measured at 298 K in Tris buffer (pH 7.4) and the phosphorescence spectra at 77 K in Tris buffer-glycerol (4:1 v/v) glassy matrix.

View Article Online
DOI: 10.1039/C7DT00291B

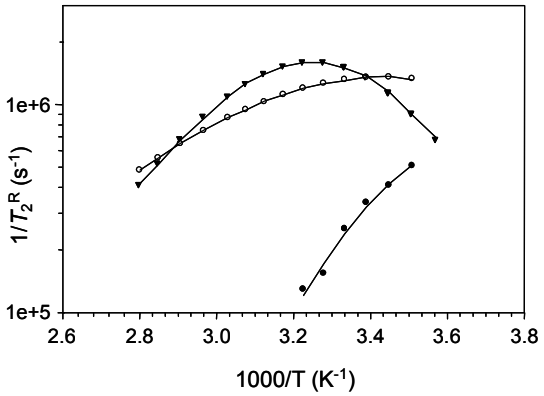

Fig. 6 Reduced transverse ^{17}O relaxation rate of water ($1/T_2^R$) for aqueous solutions of GdL^1 (closed circles) at 11.75 T, GdPCTA (open circles) and GdDOTA (closed triangles) at 7.05 T.[35a]

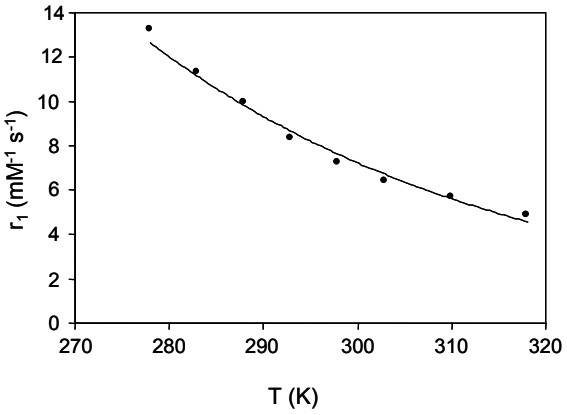

Fig. 7 Temperature (278 – 318 K) dependence of the proton longitudinal relaxivity, r_1, of GdL^1 complex in water at 20 MHz.

View Article Online
DOI: 10.1039/C7DT00291B

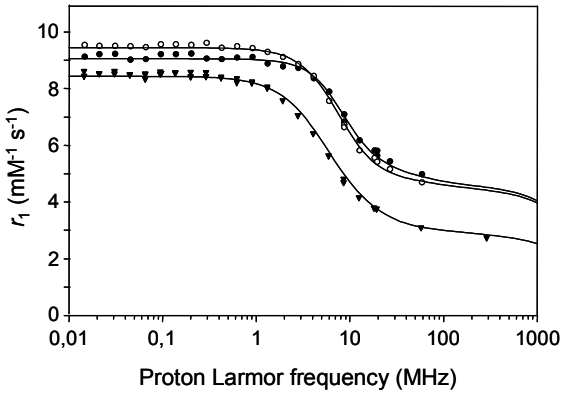

Fig. 8 Proton NMRD data obtained at 310 K on a 0.90 mM GdL^1 (closed circles), a 0.54 mM GdPCTA solution (open circles) and a 1.5 mM GdDOTA (closed triangles) solution in water. The lines correspond to the theoretical fittings.

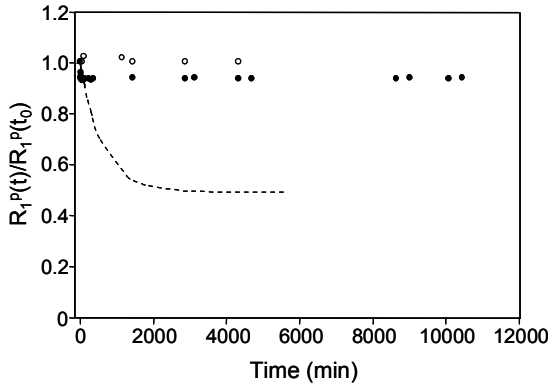

Fig. 9 Evolution of the ratio $R_1^p(t)/R_1^p(t_0)$ (T = 310 K, B_0 = 0.47 T, 20 MHz) vs. time for solutions of GdL^1 in phosphate buffer (67 mM, pH 7.0) (open circles), GdL^1 (closed circles) and GdDTPA (dashed line) in phosphate buffer containing an equimolar amount of Zn^{2+} ions.

View Article Online
DOI: 10.1039/C7DT00291B

Table 1 Absorption and metal luminescence data of TbL^1,Tb_2L^2 and related Tb complexes in aerated Tris buffer (50 mM, pH 7.4) solutions

Compd	$\pi\rightarrow\pi^*$ λ_{max}/nm (log ε)	$\tau_{H_2O}{}^a$/ms^a 298 K	$\tau_{D_2O}{}^a$/ms^a 298 K	$\tau_{D_2O}{}^a$/ms^a 77 K	q^b 298 K	$\Phi_{ov}{}^c$ (%) H_2O [D_2O]	$\Phi_{Tb}{}^d$ (%)	$\eta_{sens}{}^d$(%)
TbL^1	242 (3.81), 296 (3.48)	1.16	2.43	2.50	1.95	22 [48]	46	48
Tb_2L^2	242 (4.23), 296 (3.84)	2.02	2.48	2.60	0.16	43 [54]	78	55
[Tb(5-Me-HXTA)]$_2{}^e$	241 (4.39), 295 (4.03)	2.62	2.91	-	0.00	50	-	-
TbPCTA	269 (3.61)	1.24	2.91	3.04	2.02	8.3 [23]	41	20

[a] Determined by excitation into the lowest-energy ligand-centred absorption band and recording the intensity of the $^5D_4\rightarrow{}^7F_5$ (545 nm). [b] Number of coordinated H_2O molecules calculated using Parker equation[18] $q_{H_2O}(Tb) = 5[(\tau_{H_2O})^{-1} - (\tau_{D_2O})^{-1} - 0.06]$, with lifetimes in ms. [c] Overall quantum yield determined under ligand excitation, λ_{exc} = 296 nm. [d] Φ_{Tb} and η_{sens} are the intrinsic luminescence quantum yield and sensitization efficiency of the complexed Tb ion respectively; see text. [e] Data in water from reference 11.

Table 2 Parameters obtained from the theoretical fitting of the O-17 data for GdL^1 complex in water at 11.75 T

parameter	value
$\tau_M{}^{310K}$ [ns]	3.1 ± 0.2
$\tau_M{}^{298K}$ [ns]	9.0 ± 0.6
$\Delta H^{\neq}$ [kJ mol^{-1}]	65.5 ± 0.1
$\Delta S^{\neq}$ [J mol^{-1} K^{-1}]	129 ± 0.28
$A/\hbar$ [a] [10^6 rad s^{-1}]	-3.0
B [10^{20} s^{-2}]	8.8± 0.5
$\tau_v{}^{298K}$ [ps]	6.5 ± 0.4
E_v [a] [kJ mol^{-1}]	1

[a] Fixed parameters

Table 3 Relaxivity values at 20 MHz and parameters obtained for the theoretical fitting of the proton NMRD data in water for GdL^1 and related bis-hydrated Gd^{III} complexes (PCTA[37,42], PMNTA[6b,36d], DO3A[42], AAZTA[36f]) and clinically used GdDOTA[35].

parameter	GdL^1	GdPCTA	GdPMNTA	GdDO3A	GDAAZTA	GdDOTA
$\tau_M{}^{310K}$ [ns]	3.1 (9.0)	82 (70)	35.2 (108)	(160)	(90)	122 (244)
$\tau_R{}^{310K}$ [ps]	53 ± 1.4	56 (70)	56 (92)	(66)	(74)	53 (77)
$\tau_{SO}{}^{310K}$ [ps]	69 ± 2	129	205	-	-	404
$\tau_V{}^{310K}$ [ps]	19.4 ± 1.7	19	12.9	-	-	7
$^{20}r_1{}^{310K}$ (mM^{-1} s^{-1})	5.7 (7.2)	5.4 (6.9)	5.7	(6.0)	(7.1)	3.5 (4.7)

The values in brackets are obtained at 298 K.

View Article Online
DOI: 10.1039/C7DT00291B

New polyaminocarboxylate macrocycles containing phenolate binding units: synthesis, luminescent and relaxometric properties of their lanthanide complexes

Morgane Enel, Nadine Leygue, Stéphane Balayssac, Sophie Laurent, Chantal Galaup, Luce Vander Elst and Claude Picard

The relaxometric and (or) luminescent properties in aqueous solutions of new Ln^{III} macrocyclic complexes derived from PCTA are reported